X-551-69-323
PREPRINT

ANALYSIS OF SIGNAL AND NOISE TURNAROUND IN THE GODDARD RANGE AND RANGE RATE TRANSPONDER

T. J. GRENCHIK

AUGUST 1969

GSFC
GODDARD SPACE FLIGHT CENTER
GREENBELT, MARYLAND

X-551-69-323
PREPRINT

ANALYSIS OF SIGNAL AND NOISE TURNAROUND IN THE GODDARD RANGE AND RANGE RATE TRANSPONDER

T. J. Grenchik

August 1969

GODDARD SPACE FLIGHT CENTER
Greenbelt, Maryland

ANALYSIS OF SIGNAL AND NOISE TURNAROUND IN THE GODDARD RANGE AND RANGE RATE TRANSPONDER

T. J. Grenchik

ABSTRACT

Statistical communication theory has been used to derive the output power spectral density for a phase modulation process involving signal and noise at intermediate frequencies (bandpass modulation). The results have been applied to determine ground system capability while tracking a near earth orbiting satellite, Nimbus-E, through a synchronous satellite tracking station, ATS-F. Final results are in the form of the ground system signal to noise power densities at the essential signal component frequencies. Recommendations are made for values of transponder bandpass, modulation index, and Nimbus-E antenna gain.

SUMMARY

The process of phase modulation by an IF signal and noise has been investigated and the general equations relating the input and output spectral densities have been derived. These results are applied specifically to the situation of the Goddard Range and Range Rate (GRARR) transponder on board the Nimbus-E spacecraft relaying a tracking uplink signal through a synchronous spacecraft (ATS-F) tracking station to the ground.

From the power spectral density equations it is shown that for low phase modulation indices (0-2.0 radians) the phase modulation process causes a nearly linear translation of the IF signal and noise power densities into the RF spectral densities about the RF carrier frequency.

Based upon these results a link analysis of the tracking data relay link was performed, assuming given parameters of the tracked and data relay spacecrafts. Specific conclusions of this analysis are:

(1) Use the minimum GRARR transponder bandwidth available. The recommended value is 550 kHz.

(2) Do not use less than a 16 db transmit and a 14 db receiver Nimbus-E antenna gain. Lesser values of gain will result in increases of range rate error above ground system resolution (minimum error).

(3) A phase modulation index of approximately 1.5 radians is preferred, although this is not a critical item.

(4) The ground system noise temperature need not be extremely low since the ATS-F synchronous tracking relay station noise is dominant at the ground system input.

CONTENTS

ANALYSIS OF SIGNAL AND NOISE TURNAROUND IN THE GODDARD RANGE AND RANGE RATE TRANSPONDER

1. INTRODUCTION

In the past, when an error analysis of a spacecraft tracking system was required, it was customary to define the tracking system performance in terms of the downlink limitations alone. This attitude toward link analysis was right and proper since the uplink situation carried the advantage of the enormous transmitting systems radiating from fixed positions on earth with their surplus of primary power and temperature control capability. In contrast the cooperative transmitting system aboard a spacecraft was and is typically a thousand times less powerful than its ground counterpart. When the downlink analysis had been completed, a cursory analysis of the uplink condition usually was sufficient to complete the tracking system error analysis.

With the advent of the tracking relay satellite, it now becomes impossible to describe the tracking system limitations without considering the contexture of the uplink and downlink restrictions. (It may seem farcical to denote uplink and downlink in terms of radio links between the ground to orbiting spacecraft, and orbiting spacecraft to orbiting spacecraft, but by definition here, all radio paths from the ground via the tracking relay satellite(s) to the target spacecraft are considered to be uplink. Conversely all radio paths to the ground from the target spacecraft via the tracking relay satellite(s) are defined as the downlink.) Each of these paths or links must be investigated to determine the effect or lack of effect on the tracking measurement. In these investigations, processes which heretofore had little influence on acceptable ground tracking system operation, can be shown to produce dominant effects in the system data taking.

The purpose of this paper is the investigation of one of these processes, the phase modulation of an uplink signal upon the downlink transmission (a free running oscillator) on the target or tracked spacecraft. Specifically this target spacecraft carries a transponder called the Goddard Range and Range Rate (GRARR) transponder. This transponder is noted for its simplicity of operation since it excludes spacecraft phase lock operation and the attendant acquisition difficulties. The main text of this paper will characterize the functioning of this transponder and its ground system, and describe the influence on total system operation of the turnaround (phase modulation upon the downlink) of both uplink signal, and uplink and/or transponder noise.

The author was prompted to begin this study by the lack of readily available theoretical tools necessary for analysis of phase modulation by signal and

noise. Admittedly the necessary basic theory is present in Reference 1, 2, and 3, but the specific solutions and application to a subcarrier type of modulation system, the problem here, has not been found in the literature. In Reference 12, Abramson takes up the case of phase modulation by a Gaussian random process which has a Gaussian bandpass spectrum, and presents a simplified method of computing the spectrum of a carrier, angle modulated by this Gaussian random process. However the present study was intended to show the results of phase modulation by a signal imbedded in noise, and the author attempted to derive the solutions with as little simplifying assumption as possible. Reference 8 derives the downlink spectrum for the situation of an infinite signal to noise ratio at the GRARR transponder modulator, and in the past this reference was adequate for system analysis because the uplink signal to noise ratio remained very large under normal conditions.

The mathematical description resulting from this study of the phase modulation analysis has been applied to a potential tracking experiment scheduled for the early 1970's. In the experiment a synchronous satellite, ATS-F, will act as the relay station for the tracking transmissions to and from a 600 nautical mile circular orbit, polar orbiting satellite, Nimbus-E. From this situation it becomes apparent quickly that the uplink from ATS-F to Nimbus-E, and the downlink from Nimbus-E to ATS-F are the critical links. Even with all its weight and complexity, the ATS-F spacecraft cannot duplicate the ground station operation with its typical excess of resources. From the usage of the derived analytical tool, it is possible to show parametric requirements for GRARR transponder modulation index setting, modulation bandwidth, and effective received and transmitted power levels, in the context of a successfully executed relay tracking experiment.

2. DEFINITION OF SYMBOLS

A	peak voltage of modulator/transmitter output (volts)
B_0	peak signal drive to modulator, described in Table II and III (volts)
D_ϕ	phase modulator constant (radians/volt)
exp(x)	e^x
f_a	frequency of modulating signal, uplink translated to IF (Hz)
f_B	bandwidth of the transponder Gaussian shaped IF filter (Hz)
f_C	transponder transmitter output frequency (Hz)

f_{CF}	center frequency of the transponder IF filter (Hz)
$\mathfrak{F}$	Fourier Transform operator
I	definition of integral in section 3.3, intermediate step
$J_m (B_0 D_\phi)$	Bessel function of the first kind of integer order and argument, $B_0 D_\phi$.
$K_n (t, \tau)$	intermediate definitions used for solution of $\phi_x (t, \tau)$
N	spacecraft noise power at IF, and input to spacecraft limiter (watts)
$[n/2]$	integer value of $n/2$ after rounding off
N_o	noise output of limiter and bandpass filter, and input to modulator (watts)
N_{IN}	noise power input in Table XIII (dbm)
N_{INT}	internally generated noise power of following block, referred to input of block, in Table XIII (dbm)
N_{INC}	input noise power about the carrier (dbm)
N_{INSC}	input noise power about the subcarrier (dbm)
S	uplink signal power, translated to transponder IF, which is input to spacecraft limiter (watts)
S_C	modulator/transmitter signal power output at carrier frequency (watts)
S_{SC}	modulator/transmitter signal power output at subcarrier frequency, sum of both upper and lower spectral lines about carrier (watts)
S_G	total signal power, sum of carrier and subcarrier power, received at ground antenna output (watts)
S_{GC}	carrier signal power received at ground antenna output (watts)
S_{GSC}	subcarrier signal power received at ground antenna output, sum of both upper and lower sideband about carrier (watts)
S_{IN}	signal power input in Table XIII (dbm)

S_{INC} carrier signal power input in Table XIII (dbm)

S_{INSC} subcarrier signal power input, sum of upper and lower spectral components, in Table XIII (dbm)

S' signal output of limiter and bandpass filter, and input to modulator (watts)

$V_N(t)$ noise process defined by N_o and $\Phi(f)$, which is the drive to phase modulator (volts)

$V_S(t)$ signal drive to modulator (volts)

W noise power density of N (watts/Hz)

W' equivalent rectangular shaped noise power density at transponder IF (watts/Hz); transponder noise bandwidth = $\sqrt{2\pi}\, f_B$

$W_x(f)$ average spectral density of modulator/transmitter output (watts/Hz)

$W_x(f)_{n=0}$ average spectral density of modulator/transmitter signal output (watts/Hz)

$W_x(f)_{n\neq 0}$ average spectral density of modulator/transmitter noise output (watts/Hz)

$x(t)$ time function at input to modulator/transmitter (volts)

a_q combination of various modulating frequencies, defined by equations (63) through (67) (radians/sec)

ϵ_m Neumann factor, $\epsilon_0 = 1$, $\epsilon_m = 2$ for $m \neq 0$

Φ noise power density of N_o (watts/Hz)

Φ_C noise power density about S_C (watts/Hz)

Φ_{SC} noise power density about $S_{SC}/2$, at either upper or lower spectral line about the carrier (watts/Hz)

Φ_G ground system noise power density (watts/Hz)

Φ_{GC} noise power density about S_{GC} (watts/Hz)

Φ_{GSC} noise power density about $S_{GSC}/2$, about either upper or lower sideband about S_{GC} (watts/Hz)

$\phi_x(t, \tau)$ covariance function of nonstationary ensemble

$\phi_x(\tau)$ autocorrelation function for individual sample function, x(t)

γ_p combination of various modulating frequencies, defined by equations (50) through (54) (radians/sec)

$\varphi(\tau)$ autocorrelation function for transponder IF noise process

$\Omega(t)$ $D_\phi V_N(t) + D_\phi V_s(t)$, (radians)

$\omega_x(f)$ power spectral density for individual sample function, x(t)

3. DEFINITION OF MILIEU

Reference 7, 9, and 10 describe respectively: The Goddard Range and Range Rate Tracking System, The Goddard Range and Range Rate Transponder, and the ATS-F/NIMBUS-E data relay experiment. The interested reader may glean total detail from the perusal of these documents, but it is felt that sufficient information is presented here to avoid supplementary reading. Specifically all the reader need understand is the method of doppler extraction from the uplink and downlink transmissions, because this study only concerns itself with the doppler or range rate measurement. In the future it will be desirable to extend this study to include a concise description of the effect on the range measurement also. This requires a substantial extension of the derived theory, but preliminary estimates of the range measurement degradation can be made from the effects of modulating by an unmodulated uplink, which are included here.

3.1 GRARR Transponder Description

Figure 1 shows a functional block diagram of a GRARR transponder. Before proceeding with its description, it must be noted that the IF portion may be configured to accommodate more than one uplink signal. In Figure 1, the configuration shown is that one which will be used in the tracking experiment. The uplink signal, unmodulated for our purposes here, is received at 1800 MHz. One crystal oscillator is used within the transponder and one of its functions, after suitable multiplications, is the translation of the 1800 MHz uplink signal to a 2.4 MHz intermediate frequency. Two conversions (mixers) are used to attain the 2.4 MHz IF frequency from the 1800 MHz. The 2.4 MHz frequency is filtered in a bandpass

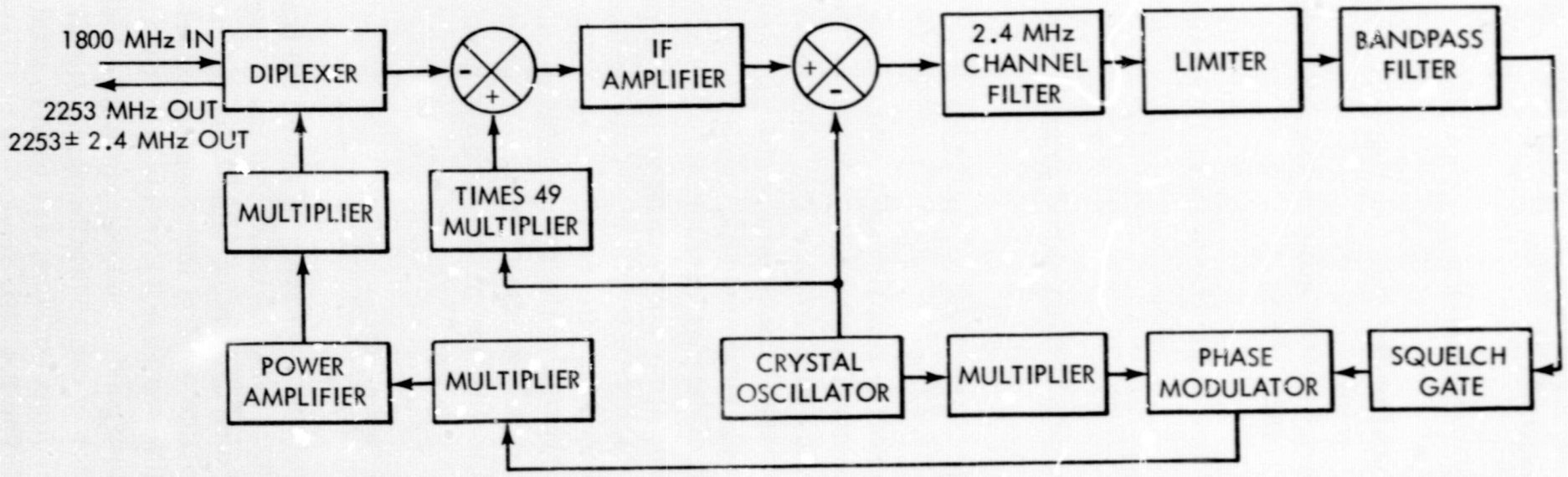

NASA-GSFC-T&DS
Mission & Trajectory Analysis Division
Branch 551 Date 8-69
By Grenchik Plot No. 1189

Figure 1-Functional Block Diagram, GRARR S-Band Transponder.

filter (2.4 MHz channel filter in Figure 1), limited, filtered again to remove harmonics, passed through a enable/disable circuit (squelch gate), and modulated on the downlink carrier at 2253 MHz, which also is generated from the single crystal oscillator within the transponder. The resulting downlink transmissions in the absence of noise are 3 primary spectral components at 2253 MHz, 2253-2.4 MHz, and 2253 + 2.4 MHz. The 2.4 MHz intermediate frequency becomes a 2.4 MHz subcarrier frequency on the 2253 MHz carrier frequency by means of the phase modulation process.

The ground tracking system which originated the uplink signal, phase locks to the downlink carrier, demodulates and phase locks to the subcarrier, and with suitable combination of the carrier, subcarrier, and ground transmitted frequencies, the ground tracking system extracts the doppler frequency caused by the rate of change of the uplink and downlink paths. That, concisely is the means of the doppler frequency or range rate extraction process.

Implied in Figure 1 is the accompanying modulation of the downlink carrier by noise, limited and shaped by the IF circuitry. The source of this noise can be internal to the transponder and/or radiated to the transponder from potential noise sources such as the ground transmitting system or the relay satellite. Origination of the noise depends upon the situation considered and in the experiment uplink, it will be predominantly GRARR transponder internal noise.

3.2 Noise Power Spectral Density Definition

At this point, some definitions are required. Define $W(f)$ as the limiter input noise spectral density in watts/Hz. In Figure 1, $W(f)$ would result from the shaping of the relatively broadband, transponder internal noise by the 2.4 MHz channel filter. It is assumed that this filter produces a Gaussian band pass spectrum, a good approximation for the output of a sharply-tuned multi-stage filter, when white noise is applied to the input. White noise, of course, is defined as noise having a spectral density uniform over the frequency band of interest.

Figure 2 presents a plot of $W(f)$, the limiter input noise spectral density produced by the 2.4 MHz channel filter shaping. $W'(f)$ is also shown in Figure 2 to illustrate the equivalent bandpass of an ideal filter which contains the same noise power, N, as the Gaussian shaped bandpass filter. This equivalent rectangular bandwidth or noise bandwidth is equal to $\sqrt{2\pi}\, f_B$. f_{CF} is defined as the center frequency of the IF filter in Hz, and for the relay experiment is equal to 2.4 MHz. f_B is a bandwidth in Hz; at $f = f_B$, the limiter input noise power spectral density, W, is down 2.17 db relative to the density at f_{CF}.

The table included at the right in Figure 2 contains the fraction of N, the total noise power contained within $3 f_B$, $4 f_B$, $5 f_B$, etc. For example, the noise

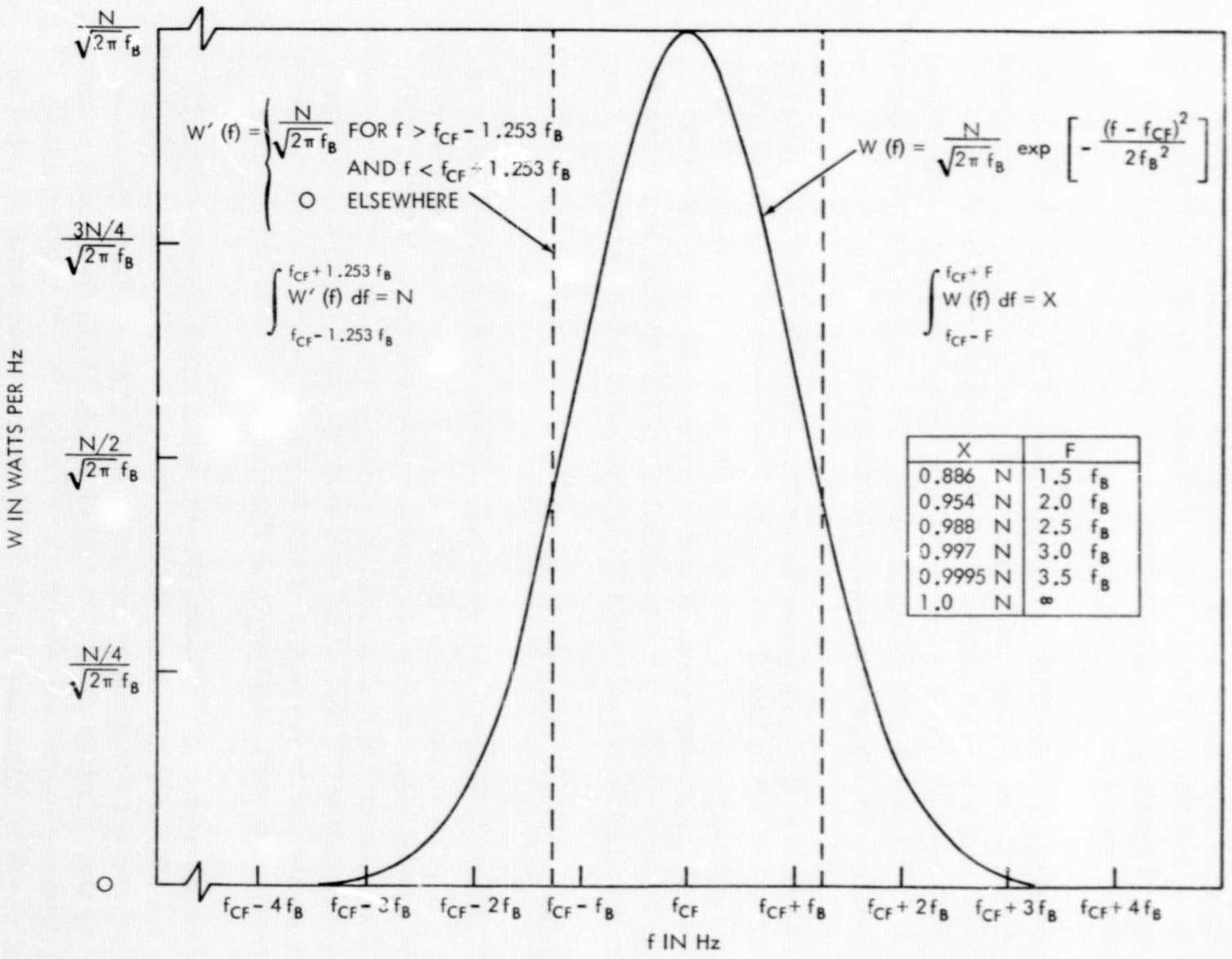

X	F
0.886 N	1.5 f_B
0.954 N	2.0 f_B
0.988 N	2.5 f_B
0.997 N	3.0 f_B
0.9995 N	3.5 f_B
1.0 N	∞

NASA-GSFC-T&DS
Mission & Trajectory Analysis Division
Branch 551 Date 8-69
By Grenchik Plot No. 1190

Figure 2-W(f), Limiter Input Noise Power Spectral Density.

power contained within the total frequency spread of 5 f_B about f_{CF} in the Gaussian shaped spectrum is equal to 98.8% of the total available IF noise power N. It will be seen later that the choice of a Gaussian shaped input filter makes the needed mathematical manipulation much more tractable. Additionally, the non-white noise power density W(f) is physically more reasonable than the ideal filter response (shown as W′(f) in Figure 2) with the abrupt transitions at $f_{CF} + \sqrt{2\pi}\, f_B/2$ and $f_{CF} - \sqrt{2\pi}\, f_B/2$.

It now remains to relate N, f_B, and S, where S is the uplink signal power in watts, translated to IF, and input to the spacecraft limiter. In the transponder, two equivalent noise bandwidths are of interest: 550 kHz and 3.9 MHz. These noise bandwidths will be considered because they meet requirements[1] for passing a "narrow" and a "wideband" uplink signal containing the ranging code. For the 550 kHz equivalent noise bandwidth, the largest ground modulation frequency used is 100 kHz, and for the 3.9 MHz equivalent noise bandwidth, the largest ground modulation frequency is 500 kHz. No further discussion will be given of the ranging modulation, except that its range of frequencies sets the minimum transponder noise bandwidth. Table I shows the calculation of parameters for the two noise bandwidths in relating them to the Gaussian bandpass filter and the uplink signal to noise ratio, S/N. The ratio $S/W(f = f_{CF})$ expresses the signal to noise power density at the translated uplink frequency, before entering the limiter. We will proceed to follow $S/W(f = f_{CF})$ through the limiter, bandpass filter, and through the modulator/transmitter, and observe the changes rendered by the nonlinear processes.

3.3 Description of Limiter Effects

In 1953 Davenport published his now-classic paper, "Signal-to-Noise Ratios in Band-Pass Limiters" in the Journal of Applied Physics (Reference 6). His paper showed that at the output of the limiter, centered about the limiter input frequencies, the output signal to noise ratio is essentially directly proportional to the input signal to noise ratio for all values of the input signal to noise ratio. However in the paper, he presents no convenient means to relate the input noise power density to the output noise power density, although one suspects that because the signal to noise ratios are essentially directly proportional, the input and output noise power densities will be related similarly. References 11 and 13[2] take up the task of relating the input and output noise spectral densities, especially near the the center frequency of the limiter operation. Tausworthe's

---

[1] Requirements are for modulation bandwidth, distortion, delay, expected oscillator drift in transponder, etc.

[2] References 11 and 13 were brought to the attention of the author by Heffernan of Goddard Space Flight Center. Mr. Heffernan also is conducting investigations in phase modulation by signal and noise.

Table I

Calculation of Signal to Noise Power Density at Transponder Limiter Input.

Equivalent Noise Bandwidth = NBW = 550 kHz		Equivalent Noise Bandwidth = NBW = 3.9 MHz	
$\frac{N}{\sqrt{2\pi}\, f_B} NBW = N$		$\frac{N}{\sqrt{2\pi}\, f_B} NBW = N$	
$f_B = \frac{550,000}{\sqrt{2\pi}} = 219,418\ Hz$		$f_B = \frac{3,900,000}{\sqrt{2\pi}} = 1,555,875\ Hz$	
$W(f) = \frac{N}{\sqrt{2\pi}\, f_B} \exp\left\{-\frac{(f - f_{CF})^2}{2 f_B^2}\right\}$		$W(f) = \frac{N}{\sqrt{2\pi}\, f_B} \exp\left\{-\frac{(f - f_{CF})^2}{2 f_B^2}\right\}$	
$W(f) = 1.818\,(10^{-6})\, N \exp\left\{\frac{-(f - f_{CF})^2}{9.629\,(10^{10})}\right\}$		$W(f) = 2.564\,(10^{-7})\, N \exp\left\{\frac{-(f - f_{CF})^2}{4.841\,(10^{12})}\right\}$	
$\frac{S}{W(f)} = \frac{\frac{S}{N}}{1.818\,(10^{-6}) \exp\left\{\frac{-(f - f_{CF})^2}{9.629\,(10^{10})}\right\}}$		$\frac{S}{W(f)} = \frac{\frac{S}{N}}{2.564\,(10^{-7}) \exp\left\{\frac{-(f - f_{CF})^2}{4.841\,(10^{12})}\right\}}$	
$\frac{S}{W(f = f_{CF})}$	$\frac{S}{N}$	$\frac{S}{W(f = f_{CF})}$	$\frac{S}{N}$
55,000,000	100	390,000,000	100
5,500,000	10	39,000,000	10
550,000	1	3,900,000	1
55,000	0.1	390,000	0.1
5,500	0.01	39,000	0.01
550	0.001	3,900	0.001

interesting conclusion is that the ratio of output signal to noise spectral density ratio to input signal to noise spectral density ratio varies between 1 and 1.16 for all values of input signal to noise ratio. At first this result seems questionable when one considers that the ratio of the output to input signal to noise ratio varies between 0.785 and 2.0.

Upon further reflection, a physical explanation of Tausworthe's results might be as follows: In the nonlinear operation of the limiter, the spectrum of the noise input tends to be broadened at the limiter output by the beating of the noise with itself and with the signal within the limiter. By summing up the total noise power at the output (centered about the limiter center frequency of operation) one may receive a slightly false impression of the effective noise spectral density because the extended tails of the noise spectrum resulting from the limiting action contribute to total noise power.

Tausworthe's results presented a quandary to the author as to how should the limiter output noise spectral density be described. The question was resolved by considering the limiter and subsequent filter to perform in either of 2 ways:

1. The output signal to noise power density is directly proportional to the output signal to noise power ratio, and Davenport's results for output S/N ratio can be applied directly to output signal to noise power density ratio.

2. The output noise power density is directly proportional to the input noise power density, and the sum of the signal and noise power at the limiter output is a constant (a slight simplification of the Tausworthe result).

Each variation of limiter and filter operation was used to calculate link degradation and these 2 solutions bound all possible solutions for any intermediate cases of limiter operation. It will be evident later that very little difference occurs between the two bounds.

Tables II and III will help to clarify the preceding paragraph. In Table II, the limiter output signal and noise power density are calculated for condition (1). The shape of the input and output noise spectrum are identical except for a change in overall amplitude. Broadening of the tails of the noise density is neglected. Where before from Table I the limiter input noise spectral density was described as:

$$W(f) = \frac{N}{\sqrt{2\pi}\, f_B} \exp\left\{ - \frac{(f - f_{CF})^2}{2 f_B^2} \right\}. \qquad (1)$$

Table II

Sample Calculation of Signal and Noise Input to Modulator with Limiter Degradation Effects Included.

D_ϕ Radians/volt	$\frac{S}{N}$	$S^*_{\substack{\text{LIMITER}\\\text{OUT}}}$ Watts	$N^*_{\substack{\text{LIMITER}\\\text{OUT}}}$ Watts	S'^{**} Watts	N_0^{**} Watts	$B_0 = \sqrt{2S'}$ Volts	Modulation Index $B_0 D_\phi$ Radians (Peak)	$\sqrt{N_0} D_\phi$ Radians (RMS)
1.5	100	$4/\pi$	$.02/\pi$	0.5	0.0025	1.0	1.5	0.0750
	10	$4/\pi$	$.2/\pi$	0.5	0.025	1.0	1.5	0.2372
	1	$2/\pi$	0.55	0.25	0.21598	0.70711	1.0607	0.6971
	0.1	0.1	1.05	0.03927	0.41233	0.28025	0.42037	0.9632
	0.01	0.01	$4/\pi$	0.003927	0.5	0.088623	0.13293	1.0607
	0.001	0.001	$4/\pi$	0.0003927	0.5	0.028025	0.04204	1.0607

*$S_{\substack{\text{LIMITER}\\\text{OUT}}}$ and $N_{\substack{\text{LIMITER}\\\text{OUT}}}$ read from Figure 4 in Reference 6.

**S' and N_0 scaled to useful values from $S_{\substack{\text{LIMITER}\\\text{OUT}}}$ and $N_{\substack{\text{LIMITER}\\\text{OUT}}}$.

the limiter output noise spectral density in watts/Hz becomes:

$$\Phi(f) = \frac{N_o}{\sqrt{2\pi}\, f_B} \exp\left\{ - \frac{(f - f_{CF})^2}{2 f_B^2} \right\} . \qquad (2)$$

Bandwidth and center frequencies remain the same, all that changes is N becomes N_o. The bandpass filter following the limiter merely removes harmonics, and $\Phi(f)$ is the noise spectral density input to the modulator. In Table II, D_ϕ is defined as the phase modulator constant in radians/volt, S′ is the signal output in watts from the limiter into the modulator, N_o is the filtered noise output (watts) of the limiter into the modulator, and B_o is the peak (not rms) voltage corresponding to the signal output power of the limiter and bandpass filter, S′. B_o is the peak signal voltage drive to the modulator. Table II was prepared from values read from Davenport's graph, relating output signal and noise power to input signal to noise ratio. S′ and N_o were scaled from Davenport's graph to useful values of modulator input.

Note in Table II, for large input signal to noise ratios to the limiter, the peak signal voltage output, B_o, multiplied by the modulator constant, D_ϕ, results in a peak modulator drive of 1.5 radians. At a signal to noise ratio input of 0.001, the effective peak signal modulator drive is only 0.04204 radians, but now the effective RMS drive from the noise, $\sqrt{N_o}\, D_\phi$, results in a RMS radian change of 1.0607 radians. At large input signal to noise ratios the signal drives the modulator, at low input signal to noise ratio the noise drives the modulator.

Table III has been prepared in illustration of condition (2), a simplification of Tausworthe's results. Here it is assumed that the shape of the output noise spectral density remains unchanged as under condition (1), that is[3]:

$$\Phi(f) = \frac{N_o}{\sqrt{2\pi}\, f_B} \exp\left\{ \frac{- (f - f_{CF})^2}{2 f_B^2} \right\} \qquad (2)$$

but a different method is used to calculate N_o from S and N. Definitions for $\Phi(f)$ and N_o remain the same, only their numerical values change slightly. Output power of the limiter/bandpass filter is a constant .505 watts with the

[3]Tausworthe's results imply noise spectrum broadening, but it is assumed here that the bandpass filter skirts remove the broadened part of the spectrum and restore the noise spectral density at the output to the same form as at the limiter input. The simplification here is assuming no signal to noise power density degradation occurs for any input signal to noise ratio.

Table III

Sample Calculation of Signal and Noise Input to Modulator with No Limiter Degradation Effects Included.

D_ϕ Radians/volt	$\frac{S}{N}$	$S' + N_o$ Watts	S' Watts	N_o Watts	$B_o = \sqrt{2S'}$ Volts	Mod. Index $B_o D_\phi$ Radians (Peak)	$\sqrt{N_o} D_\phi$ Radians (RMS)
1.5	100	.505	0.5	0.005	1.0	1.5	0.10606
	10		0.45909	0.045909	0.9582	1.437	0.3214
	1		0.2525	0.2525	0.7106	1.066	0.7537
	0.1		0.045909	0.45909	0.3030	0.4545	1.0163
	0.01		0.005	0.5	0.1000	0.1500	1.0607
	0.001		0.000504	0.504495	0.03176	0.0476	1.0654

apportioning of power to signal and noise set by the input signal to noise ratio to the limiter. Just as under condition (1), it can be seen that the modulator drive is mostly signal for large S/N, and mostly noise for low S/N.

4. DERIVATION OF PHASE MODULATOR OUTPUT POWER SPECTRUM

Up to this point, the assumptions have been set down leading to the definition of the signal and noise structure at the input to the GRARR transponder phase modulator/transmitter. It is at this point that the important derivation is made for the output power spectral density of the phase modulator/transmitter when an unmodulated signal and noise (as defined in section 2.3) are the input.

4.1 Definition of Method[4]

One must begin with definition of symbols so that an orderly presentation of results can follow. We have a function of time, $x(t)$, at the output of the modulator/transmitter which has been assumed to be a combination of a periodic function (an unmodulated sinusoid), and a random function described by total power, N_o, and a Gaussian shaped power spectral density (Equation 2). The

[4] As preliminary background, the reader unversed in statistical communication theory should read Reference 5 for definition of the mathematical processes expressed in engineering language. As further background he should also read pgs. 35 to 39 of Reference 1.

covariance of this random process consisting of signal and noise is defined as

$$\phi_x(t, \tau) = \langle x(t+\tau)\, x^*(t) \rangle \tag{3}$$

where $\langle\ \rangle$ indicates expected or average value of the enclosed function and the symbol * indicates the complex conjugate. The covariance function $\phi_x(t, \tau)$ is shown as a function of time, t, and time difference, τ, because the function $x(t)$ may be a sample function from a nonergodic (nonstationary) ensemble and, the probability densities derived from each sample function, $x(t)$, are dependent upon the origin from which time was measured.

The spectral density of the ensemble $W_x(f)$, the output of the phase modulator/transmitter and the desired result, is defined as the average spectral density of the individual sample functions

$$W_x(f) = \langle \omega_x(f) \rangle \tag{4}$$

where the autocorrelation function for an individual sample function, $x(t)$, is defined as the time average

$$\phi_x(\tau) = \overline{x(t+\tau)\, x^*(t)} = \lim_{T \to \infty} \frac{1}{2T} \int_{-T}^{T} x(t+\tau)\, x^*(t)\, dt \tag{5}$$

and

$$\omega_x(f) = \int_{-\infty}^{\infty} \phi_x(\tau) \exp(-j\, 2\pi\, f\tau)\, d\tau \tag{6}$$

$$\phi_x(\tau) = \int_{-\infty}^{\infty} \omega_x(f) \exp(j\, 2\pi\, f\tau)\, df\ . \tag{7}$$

Equations (6) and (7) are the Fourier transform pair relating the individual sample function, $x(t)$, its autocorrelation, $\phi_x(\tau)$, and its power spectral density $\omega_x(f)$.

To solve Equation (4) we take the expected value of Equation (6)

$$W_x(f) = \langle \omega_x(f) \rangle = \left\langle \int_{-\infty}^{\infty} \phi_x(\tau) \exp(-j\,2\pi f\tau)\, d\tau \right\rangle . \tag{8}$$

By assuming that the expected value operation can be done inside the integral, one has

$$W_x(f) = \langle \omega_x(f) \rangle = \int_{-\infty}^{\infty} \langle \phi_x(\tau) \rangle \exp(-j\,2\pi f\tau)\, d\tau . \tag{9}$$

Similarly by taking the expected value of Equation (7) one has

$$\langle \phi_x(\tau) \rangle = \int_{-\infty}^{\infty} \langle \omega_x(f) \rangle \exp(j\,2\pi f\tau)\, df . \tag{10}$$

Equations (9) and (10) are the Fourier transform pair relating the expected value of the autocorrelation function and the expected value of the power spectral density for the sample function $x(t)$. From Equations (9) and (10) we have

$$W_x(f) = \langle \omega_x(f) \rangle = \mathfrak{F}\langle \phi_x(\tau) \rangle \tag{11}$$

where $\mathfrak{F}$ denotes the Fourier transform operation.

Now if it is assumed that time and ensemble averages may be interchanged, then

$$\langle \phi_x(\tau) \rangle = \overline{\phi_x(t, \tau)} = \lim_{T \to \infty} \frac{1}{2T} \int_{-T}^{T} \phi_x(t, \tau)\, dt \tag{12}$$

where $\overline{\phi_x(t, \tau)}$ is the time average of $\phi_x(t, \tau)$, and

$$W_x(f) = \mathfrak{F}\left[\overline{\phi_x(t, \tau)}\right] . \tag{13}$$

Equation (13) is the desired result relating the average spectral density, $\mathbb{W}_x(f)$, of the ensemble defined in Equation (8), to the Fourier transform of the average covariance, $\overline{\phi_x(t,\tau)}$, of the non-stationary ensemble.

4.2 Application of Method

The application of the method of 4.1 follows directly. Define the output voltage of the modulator/transmitter to be:

$$x(t) = A\cos\left[2\pi f_C t + D_\phi V_N(t) + D_\phi V_S(t)\right] \tag{14}$$

where A is the peak voltage of the modulator/transmitter output ($A_0^2/2$ = total available power), f_C is the transmitter center frequency (2253 MHz), $V_N(t)$ is the random process defined by N_0 and $\Phi(f)$, D_ϕ, already defined, is the phase modulator constant, and

$$V_S(t) = B_0\cos 2\pi f_a t \tag{15}$$

$V_S(t)$ is the signal drive to the modulator in volts, B_0 is the peak signal drive (see Table II or III), and f_a is the frequency of the modulating signal in Hz. f_a is the uplink frequency, translated to IF within the transponder (2.4 MHz), which modulates the phase modulator/transmitter.

The calculation of $\phi_x(t,\tau)$ follows the definition of $x(t)$:

$$\phi_x(t,\tau) = \langle A\cos\left[2\pi f_c(t+\tau) + D_\phi V_N(t+\tau) + D_\phi V_S(t+\tau)\right] \times A\cos\left[2\pi f_C t + D_\phi V_N(t) + D_\phi V_S(t)\right]\rangle . \tag{16}$$

Let

$$\Omega(t) = D_\phi V_N(t) + D_\phi V_S(t) . \tag{17}$$

Then

$$\phi_x(t,\tau) = A^2\langle\cos\left[2\pi f_C(t+\tau) + \Omega(t+\tau)\right]\cos\left[2\pi f_C t + \Omega(t)\right]\rangle . \tag{18}$$

By the law of cosines,

$$\cos A \cos B = \frac{1}{2}\left[\cos (A + B) + \cos (A - B)\right] ,$$

$$\phi_x (t, \tau) = \frac{A^2}{2} \left\langle \cos \left[4\pi f_c t + 2\pi f_c \tau + \Omega(t + \tau) + \Omega(t)\right]\right.$$

$$\left. + \cos \left[2\pi f_c \tau + \Omega(t + \tau) - \Omega(t)\right]\right\rangle \cdot \quad (19)$$

It is convenient to write Equation (19) in exponential form:

$$\phi_x (t, \tau) = \frac{A^2}{2} \left\langle \mathrm{Re} \exp\left\{j \left[4\pi f_c t + 2\pi f_c \tau + \Omega(t + \tau) + \Omega(t)\right]\right\}\right\rangle$$

$$+ \frac{A^2}{2} \left\langle \mathrm{Re} \exp\left\{j \left[2\pi f_c \tau + \Omega(t + \tau) - \Omega(t)\right]\right\}\right\rangle \cdot \quad (20)$$

At this point we wish to examine only:

$$\left\langle \exp\left\{j \left[\Omega(t + \tau) - \Omega(t)\right]\right\}\right\rangle . \quad (21)$$

Define this function as $K_1 (t, \tau)$, an intermediate step in the solution for $\phi_x (t, \tau)$. From (17)

$$K_1 (t, \tau) = \left\langle \exp\left\{j D_\phi \left[V_N (t + \tau) + V_S (t + \tau) - V_N (t) - V_S (t)\right]\right\}\right\rangle . \quad (22)$$

It has been assumed that the signal and noise at the input to the modulator are independent of each other, thus

$$K_1 (t, \tau) = \left\langle \exp\left\{j D_\phi \left[V_N (t + \tau) - V_N (t)\right]\right\}\right\rangle \left\langle \exp\left\{j D_\phi \left[V_S (t + \tau)\right.\right.\right.$$

$$\left.\left.\left. - V_S (t)\right]\right\}\right\rangle . \quad (23)$$

From Reference 1, page 34 using Rowe's solution for the joint characteristic function, we have for the first average of $K_1(t, \tau)$

$$\left\langle \exp\left\{ j D_\phi \left[V_N(t+\tau) - V_N(t) \right] \right\} \right\rangle = \exp\left\{ - D_\phi^2 \left[\varphi(0) - \varphi(\tau) \right] \right\} \qquad (24)$$

where $\varphi(0)$ is the autocorrelation function for the modulating noise process with $\tau = 0$, and $\varphi(\tau)$ is the autocorrelation function with τ as a variable.

From Reference 5, page 626, the autocorrelation function for a Gaussian bandpass spectrum is given as

$$\varphi(\tau) = N_o \exp\left[\frac{-(2\pi f_B \tau)^2}{2} \right] \cos 2\pi f_{CF} \tau \qquad (25)$$

and for $\tau = 0$

$$\varphi(0) = N_o . \qquad (26)$$

Combining Equations (24), (25), and (26), one arrives at

$$\left\langle \exp\left\{ j D_\phi \left[V_N(t+\tau) - V_N(t) \right] \right\} \right\rangle = \exp\left\{ - D_\phi^2 N_o \left[1 - \exp\left(j \sqrt{2}\pi f_B \tau \right)^2 \cos 2\pi f_{CF} \tau \right] \right\} . \qquad (27)$$

Now examine the second average of $K_1(t, \tau)$

$$\left\langle \exp\left\{ j D_\phi \left[V_S(t+\tau) - V_S(t) \right] \right\} \right\rangle = \sum_{m=0}^{\infty} \epsilon_m J_m^2 \left(B_c D_\phi \right) \cos m 2\pi f_a \tau . \qquad (28)$$

Equation (28) has been derived by Middleton (Reference 2) on page 612, and used here with B_0, D_ϕ, and f_a already defined in terms of the transponder signal modulation process. $J_m(B_0 D_\phi)$ is a Bessel function of the 1st kind of integer order. ϵ_m is

the Neumann factor with

$$\epsilon_0 = 1 \tag{29}$$

$$\epsilon_m = 2, \qquad m \neq 0. \tag{30}$$

Equation 20 now becomes

$$\phi_x(t, \tau) = \frac{A^2}{2} \left\langle \mathrm{Re} \exp \left\{ j \left[4\pi f_c t + 2\pi f_c \tau + \Omega(t+\tau) + \Omega(t) \right] \right\} \right\rangle$$

$$+ \frac{A^2}{2} \mathrm{Re} \left[K_1(\tau) \exp\left(j\, 2\pi f_c \tau \right) \right] . \tag{31}$$

Note that $K_1(t, \tau)$ has become a function of τ alone, so that it may be expressed as $K_1(\tau)$ in Equation (31). Similarly in Equation 31, it can be shown by the preceding method that

$$\left\langle \exp \left\{ \Omega(t+\tau) + \Omega(t) \right\} \right\rangle = K_2(\tau) \tag{32}$$

where $K_2(\tau)$ is another function dependent upon τ only. It will be evident shortly that a complete solution for $K_2(\tau)$ is not required because it is contained within a term that goes to zero. Equation (31) upon simplification is:

$$\phi_x(t, \tau) = \frac{A^2}{2} \mathrm{Re} \left\{ K_2(\tau) \exp \left[j\left(4\pi f_c t + 2\pi f_c \tau \right) \right] \right\}$$

$$+ \frac{A^2}{2} \mathrm{Re} \left\{ K_1(\tau) \exp \left[j\, 2\pi f_c \tau \right] \right\} . \tag{33}$$

The next step required, as outlined in section 4.1 calls for taking the ensemble average, $\langle\ \rangle$, by means of the time average of Equation (33)

$$\overline{\phi_x(t, \tau)} = \lim_{T \to \infty} \frac{1}{2T} \int_{-T}^{T} \phi_x(t, \tau)\, dt = \langle \phi_x(t, \tau) \rangle \tag{34}$$

$$\overline{\phi_x(t,\tau)} = \frac{A^2}{2}\,\mathrm{Re}\left\{K_2(\tau)\exp\left[j\,2\pi f_c \tau\right]\lim_{T\to\infty}\frac{1}{2T}\int_{-T}^{T}\exp\left[j\,4\pi f_c t\right]dt\right\}$$

$$+\frac{A^2}{2}\,\mathrm{Re}\left\{K_1(\tau)\exp\left[j\,2\pi f_c \tau\right]\right\}. \quad (35)$$

The integral within the first term of Equation (35) is zero, that is

$$\lim_{T\to\infty}\frac{1}{2T}\int_{-T}^{T}\exp\left[j\,4\pi f_c t\right]dt = \lim_{T\to\infty}\frac{\sin 4\pi f_c T}{4\pi f_c T} = 0 \quad \text{for} \quad f_c \neq 0. \quad (36)$$

Equation (35) becomes after this simplification:

$$\overline{\phi_x(t,\tau)} = \frac{A^2}{2}\,\mathrm{Re}\left\{K_1(\tau)\exp\left[j\,2\pi f_c \tau\right]\right\} \quad (37)$$

and with removal of the exponential form

$$\overline{\phi_x(t,\tau)} = \frac{A^2}{2}K_1(\tau)\cos 2\pi f_c \tau\,. \quad (38)$$

with $K_1(\tau)$ defined by Equations (27) and (28)

$$K_1(\tau) = \exp\left\{-D_\phi^2 N_o\left[1-\exp\left(j\sqrt{2}\pi f_B \tau\right)^2\cos 2\pi f_{CF}\tau\right]\right\}\sum_{m=0}^{\infty}\epsilon_m J_m^2\left(B_o D_\phi\right)$$

$$\times \cos m\,2\pi f_a \tau\,. \quad (39)$$

Finally from Equation (13), $W_x(f)$, the average spectral density, can be solved for by the Fourier transform of $\overline{\phi_x(t,\tau)}$. Note that $\overline{\phi_x(t,\tau)}$ is no longer a function of time after the time averaging.

$$W_x(f) = \int_{-\infty}^{\infty} \overline{\phi_x(t,\tau)} \exp(-j\,2\pi f\tau)\, d\tau = \int_0^{\infty} 4\,\overline{\phi_x(t,\tau)} \cos 2\pi f\tau\, d\tau \ . \quad (40)$$

Combining Equations (38), (39), and (40), we have the expression for the average power spectral density of the phase modulator/transmitter output, expressed in integral form:

$$W_x(f) = \int_0^{\infty} 4\cos 2\pi f\tau \left[\frac{A^2}{2}\cos 2\pi f_C\tau\right] \exp\left\{-D_\phi^2 N_o\left[1-\exp\left(j\sqrt{2}\pi f_B\tau\right)^2 \times \cos 2\pi f_{CF}\tau\right]\right\} \sum_{m=0}^{\infty}\left[\epsilon_m J_m^2(B_o D_\phi)\cos m\,2\pi f_a\tau\right] d\tau \ . \quad (41)$$

4.3 Solution of the Integral $W_x(f)$

The infinite summation contained within the integral of Equation (41) has values for the peak amplitudes of each term in m expressed as the square of Bessel functions of the first kind of integer order. The argument $B_o D_\phi$, from practical limitations, will be no larger than 2.0. To show the rapid convergence of this infinite series for arguments less than 2.0, Table 4 lists values of $J_m^2(B_o D_\phi)$ for various values of m and for $B_o D_\phi$ less than 2.0. For our purpose here we shall truncate the series at m = 6. This allows the integral $W_x(f)$ to be expressed as

$$W_x(f) = 2A^2 \exp(-D_\phi^2 N_o) \sum_{m=0}^{6} \epsilon_m J_m^2(B_o D_\phi) \int_0^{\infty} (\cos 2\pi f\tau)(\cos 2\pi f_C\tau) \times (\cos m\,2\pi f_a\tau) \exp\left[\left(D_\phi^2 N_o \cos 2\pi f_{CF}\tau\right) \exp\left(j\sqrt{2}\pi f_B\tau\right)^2\right] d\tau \ . \quad (42)$$

Table IV

Illustration of Convergence of Bessel Function Series for $B_o D_\phi$ Less Than 2.0.

$$\sum_{m=0}^{\infty} \epsilon_m J_m^2 (B_o D_\phi) \cos m 2\pi f_a \tau = J_0^2 (B_o D_\phi) + 2 J_1^2 (B_o D_\phi) \cos 2\pi f_a \tau$$

$$+ 2 J_2^2 (B_o D_\phi) \cos 4\pi f_a \tau + 2 J_3^2 (B_o D_\phi) \cos 6\pi f_a \tau$$

$$+ 2 J_4^2 (B_o D_\phi) \cos 8\pi f_a \tau + 2 J_5^2 (B_o D_\phi) \cos 10\pi f_a \tau + \cdots$$

$J_m^2 (B_o D_\phi)$

Modulation Index	m = 0	m = 1	m = 2	m = 3	m = 4	m = 5
$B_o D_\phi = 0.5$	.88073	.05869	.00094	.00001	$3\ (10^{-8})$	
$B_o D_\phi = 1.0$	.58553	.19364	.01320	.00038	.00001	$6\ (10^{-8})$
$B_o D_\phi = 1.5$	.26197	.31129	.05386	.00372	.00014	$3\ (10^{-6})$
$B_o D_\phi = 2.0$	.05013	.33261	.12449	.01663	.00116	.00005

Now expand the exponential function in a power series:

$$\exp \left[\left(D_\phi^2 N_o \cos 2\pi f_{CF} \tau \right) \exp \left(j \sqrt{2} \pi f_B \tau \right)^2 \right]$$

$$= \sum_{n=0}^{\infty} \frac{D_\phi^{2n} N_o^n}{n!} \cos^n 2\pi f_{CF} \tau \exp \left[- n \left(\sqrt{2} \pi f_B \tau \right)^2 \right] . \quad (43)$$

The series in Equation (43) is uniformly convergent over $[0, \infty]$ and the summation sign of Equation (43) can be placed outside the integral.

$$W_x(f) = 2A^2 \exp\left(-D_\phi^2 N_o\right) \sum_{m=0}^{6} \sum_{n=0}^{\infty} \epsilon_m J_m^2 \left(B_o D_\phi\right) \frac{D_\phi^{2n} N_o^n}{n!} \int_0^\infty (\cos 2\pi f\tau)$$

$$(\cos 2\pi f_C \tau)(\cos m\, 2\pi f_a \tau)(\cos 2\pi f_{CF} \tau)^n \exp\left[-n\left(\sqrt{2}\pi f_B \tau\right)^2\right] d\tau \quad . \quad (44)$$

Here we look at only the integral, defined as I,

$$I = \int_0^\infty (\cos 2\pi f\tau)(\cos 2\pi f_C \tau)(\cos m\, 2\pi f_a \tau)(\cos 2\pi f_{CF} \tau)^n$$

$$\exp\left[-n\left(\sqrt{2}\pi f_B \tau\right)^2\right] d\tau . \quad (45)$$

The one term in the integral which still prevents facile integration is $(\cos 2\pi f_{CF}\tau)^n$. It can be shown that this function can be expressed as a finite sum of terms for an integer $n \geq 0$:

$$(\cos 2\pi f_{CF}\tau)^n = \frac{1}{2^n} \sum_{k=0}^{[n/2]} \frac{n!\,\epsilon_{n-2k}}{k!(n-k)!} \cos(n-2k)\, 2\pi f_{CF}\tau \quad (46)$$

ϵ_{n-2k} is the Neumann factor with

$$\epsilon_0 = 1 \quad (47)$$

$$\epsilon_r = 2 \qquad (r \neq 0) . \quad (48)$$

$\frac{n!}{k!(n-k)!}$ is the binomial coefficient $\binom{n}{k}$ and $[n/2]$ is the integer value of $n/2$ after rounding off.

I, the integral now becomes

$$I = \frac{1}{2^n} \sum_{k=0}^{[n/2]} \frac{n!\ \epsilon_{n-2k}}{k!(n-k)!} \int_0^\infty [\cos 2\pi f\tau][\cos 2\pi f_c \tau][\cos m\, 2\pi f_a \tau]$$

$$[\cos (n-2k)\, 2\pi f_{CF} \tau] \exp\left[-n\left(\sqrt{2}\pi f_B \tau\right)^2\right] d\tau \quad .(49)$$

Let

$$2\pi f_c = A \quad (50)$$

$$m\, 2\pi f_a = B \quad (51)$$

$$2\pi f = C \quad (52)$$

$$(n-2k)\, 2\pi f_{CF} = D\,. \quad (53)$$

Then

$$[\cos A\tau][\cos B\tau][\cos C\tau][\cos D\tau]$$

$$= \frac{1}{8}\{\cos (A+B+C+D)\tau + \cos (A+B-C-D)\tau + \cos (A+B+C-D)\tau$$

$$+ \cos (A+B-C+D)\tau + \cos (A-B+C+D)\tau + \cos (A-B-C-D)\tau$$

$$+ \cos (A-B+C-D)\tau + \cos (A-B-C+D)\tau\} = \frac{1}{8}\sum_{p=1}^{8} \cos \gamma_p \tau \quad (54)$$

where the γ_p's are defined by Equations 50 through 54. Equation (49) now becomes

$$I = \frac{1}{2^n} \sum_{k=0}^{[n/2]} \sum_{p=1}^{8} \frac{n!\, \epsilon_{n-2k}}{8k!(n-k)!} \int_0^\infty \exp\left[-n\left(\sqrt{2}\pi f_B \tau\right)^2\right] \cos \gamma_p \tau \, d\tau \,. \quad (55)$$

From definite integral tables, one finds

$$\int_0^\infty \exp\left(-a^2 x^2\right) \cos bx \, dx = \frac{\sqrt{\pi} \exp\left(-\frac{b^2}{4a^2}\right)}{2a} \quad [a > 0] \,. \quad (56)$$

Upon application of this integral solution to I, I becomes

$$I = \frac{1}{2^n} \sum_{k=0}^{[n/2]} \sum_{p=1}^{8} \frac{n!\, \epsilon_{n-2k}}{8k!(n-k)!} \left\{ \frac{1}{2\sqrt{2\pi n}\, f_B} \exp\left[\frac{-\gamma_p^2}{8n\pi^2 f_B^2}\right] \right\} \quad (57)$$

with the restrictions that $n > 0$. This restriction will be removed shortly.

Equation (57) simplifies slightly to

$$I = \frac{n!}{\sqrt{n\pi}\, 2^{n+9/2} f_B} \sum_{k=0}^{[n/2]} \sum_{p=1}^{8} \frac{\epsilon_{n-2k}}{k!(n-k)!} \exp\left[\frac{-\gamma_p^2}{8n\pi^2 f_B^2}\right] \quad (58)$$

still with the restriction that $n > 0$. The implication of this restriction is, at $n = 0$ the resulting Equation (44) represents the values of the signal components in the spectrum. For $n \geq 1$ in Equation (44), the results represent the noise power spectral density after the modulation process. To evaluate $W_x(f)$ at

$n = 0$ it is convenient to express Equation (44) as

$$W_x(f) = \sum_{m=0}^{6} \sum_{n=0}^{\infty} K_3 \frac{D_\phi^{2n} N_o^n}{n!} \int_0^\infty (\cos 2\pi f\tau)(\cos 2\pi f_C \tau)(\cos m 2\pi f_a \tau)$$

$$\times (\cos 2\pi f_{CF} \tau)^n \exp\left[-n\left(\sqrt{2}\pi f_B \tau\right)^2\right] d\tau \quad (59)$$

where K_3 represents all terms not dependent on n. Now from Equation (46)

$$(\cos 2\pi f_{CF} \tau)^n = \frac{1}{2^n}\left[\epsilon_n \cos n 2\pi f_{CF} \tau + n \epsilon_{n-2} \cos (n-2) 2\pi f_{CF} \tau\right.$$

$$\left. + \frac{n(n-1)}{2!} \epsilon_{n-4} \cos (n-4) 2\pi f_{CF} \tau + \cdots\right] \quad (60)$$

and at n equal to zero, $(\cos 2\pi f_{CF} \tau)^n$ becomes

$$\epsilon_0 \cos 0 = 1 . \quad (61)$$

The factor $\exp\left[-n\left(\sqrt{2}\pi f_B \tau\right)^2\right]$ equals 1 at $n = 0$ so that

$$W_x(f)_{n=0} = \sum_{m=0}^{6} K_3 \int_0^\infty (\cos 2\pi f\tau)(\cos 2\pi f_C \tau)(\cos m 2\pi f_a \tau)\, d\tau . \quad (62)$$

Recall that we defined

$$2\pi f_C = A \quad (63)$$

$$m 2\pi f_a = B \quad (64)$$

$$2\pi f = C \tag{65}$$

and

$$(\cos A\tau)(\cos B\tau)(\cos C\tau) = \frac{1}{4}\cos(A+B+C)\tau + \frac{1}{4}\cos(A+B-C)\tau$$

$$+ \frac{1}{4}\cos(A-B+C)\tau + \frac{1}{4}\cos(A-B-C)\tau \tag{66}$$

$$= \frac{1}{4}\sum_{q=1}^{4}\cos\alpha_q\tau\ . \tag{67}$$

Then

$$W_x(f)_{n=0} = \sum_{m=0}^{6}\sum_{q=1}^{4}\frac{K_3}{4}\int_0^\infty \cos\alpha_q\tau\,d\tau\ . \tag{68}$$

The integral of Equation (68) results in the impulse function,

$$\int_0^\infty \cos 2\pi ft\,dt = \frac{1}{2}\delta(f) \tag{69}$$

where $\delta(f)$ is an even unit impulse function.

Equation (68) becomes

$$W_x(f)_{n=0} = \sum_{m=0}^{6}\sum_{q=1}^{4}\frac{K_3}{4}\frac{1}{2}\delta(\alpha_q)\ . \tag{70}$$

Writing out the terms of the α_q series in Equation (70) we have

$$W_x(f)_{n=0} = \sum_{m=0}^{6} \frac{K_3}{8} \left[\delta\left(2\pi f_c + m\,2\pi f_a + 2\pi f\right) + \delta\left(2\pi f_c + m\,2\pi f_a - 2\pi f\right) \right.$$

$$\left. + \delta\left(2\pi f_c - m\,2\pi f_a + 2\pi f\right) + \delta\left(2\pi f_c - m\,2\pi f_a - 2\pi f\right) \right] \quad . (71)$$

We must remember that $2\pi f_c$ and $2\pi f_a$ are greater than zero (they are real frequencies) and $2\pi f$ can only be equal to or greater than zero in the integral

$$\int_0^\infty \cos \alpha_q \tau \, d\tau \, .$$

This means that

$$\left(2\pi f + 2\pi f_c + m\,2\pi f_a\right) > 0 \qquad (72)$$

$$\left(2\pi f + 2\pi f_c - m\,2\pi f_a\right) > 0 \qquad (73)$$

and

$$\left.\begin{array}{l} \delta\left(2\pi f + 2\pi f_c + m\,2\pi f_a\right) \\ \delta\left(2\pi f + 2\pi f_c - m\,2\pi f_a\right) \end{array}\right\} \text{are always equal to zero.} \qquad (74)$$

With this restriction we arrive at

$$W_x(f)_{n=0} = \sum_{m=0}^{6} \frac{K_3}{8} \left[\delta\left(2\pi f_C + m\,2\pi f_a - 2\pi f\right) + \delta\left(2\pi f_C - m\,2\pi f_a - 2\pi f\right)\right] . \quad (75)$$

With the reinsertion of the value for K_3, Equation (75) becomes

$$W_x(f)_{n=0} = \sum_{m=0}^{\infty} \frac{A^2}{4} \exp\left(-D_\phi^2 N_o\right) \epsilon_m J_m^2\left(B_o D_\phi\right) \left[\delta\left(2\pi f_C + m\,2\pi f_a - 2\pi f\right) + \delta\left(2\pi f_C - m\,2\pi f_a - 2\pi f\right)\right] \quad (76)$$

and Equation (76) states the resulting signal power spectrum as a function of signal and noise. If the noise power into the modulator is zero, $\exp\{-D_\phi^2 N_o\}$ equals 1 and Equation (76) reduces to the usual method of calculating signal power in the carrier ($f = f_C$), the subcarrier, ($f = f_C - f_a$ and $f = f_C + f_a$), and higher order terms ($f = f_C + m f_a$, $f = f_C - m f_a$).

At Equation (58), we digressed to the solutions of $W_x(f)$ only for the signal components of the spectrum. At that time, however, the solution existed (in fragments) for the noise power spectral density. Here we put the fragments together. We can remove the restriction that $n > 0$ by deleting $n = 0$ from the summation, since we have already solved for it as the signal spectrum. We

combine here Equations (44) and (58)

$$W_x(f)_{n\neq 0} = \frac{A^2}{\sqrt{\pi}\, 2^{7/2} f_B} \exp\left(-D_\phi^2 N_o\right) \sum_{m=0}^{6} \sum_{n=1}^{\infty} \sum_{k=0}^{[n/2]} \sum_{p=1}^{8} \frac{\epsilon_m J_m^2\left(B_o D_\psi\right) D_\phi^{2n} N_o^n}{\sqrt{n}\, 2^n k!(n-k)!} \epsilon_{n-2k} \exp\left(\frac{-\gamma_p^2}{8n\pi^2 f_B^2}\right) \quad (77)$$

to arrive at the expression for the noise power spectral density at the output of the phase modulator/transmitter. Equations (76) and (77) are the desired result but unfortunately the physical picture has been lost in the mire of algebra. The author was forced to automate the calculation of these functions in order to present meaningful results (which are strongly lacking when one views Equations (76) and especially (77)). Pictorial results will be shown in the following section so that the strength of this analytical tool may be made more clear.

5. NUMERICAL RESULTS—TRANSPONDER SIGNAL AND NOISE OUTPUT

The solution for Equations (76) and (77) requires a large amount of calculation, and it was obvious that machine computation was required. Preceding sections had already defined all parameters needed for the calculation (i.e., Table I, II and III), except for A, the peak amplitude of the transponder output voltage. It was convenient to make $A = \sqrt{2}$, in order to normalize the total available transponder output power at 1 watt. With this final parameter defined, the calculation of numerical results followed the machine execution of a program developed by Mr. C. W. Murray of Goddard Space Flight Center. This program maintains as variable parameters: A, D_ϕ, N_o, B_o, f_B, f_C, f_a, and f_{CF} so that various conditions can be assumed for the transponder input signal and noise. Recall however that the transponder limiter input noise power spectral density is assumed Gaussian shaped, and that the modulator input noise power spectral density retains the same shape and is assumed uncorrelated with the unmodulated signal input to the modulator.

Additionally Tables II and III which show calculations for N_o, B_o as function of S/N at the limiter input, assume that the transponder "hard" limits on transponder noise even in the absence of a signal. Thus the input to the modulator

remains essentially a constant for all values of S/N [5] whether it be predominantly signal or predominantly noise or intermediate combinations.

Table I shows the calculation of signal to noise power density at the limiter input for two values of transponder noise bandwidth, $\sqrt{2\pi}\, f_B$ = 550 kHz or 3900 kHz. From practical considerations (ranging code bandwidths), these 2 values of f_B will be the only ones considered further here, although the program will accommodate any reasonable f_B.

D_ϕ, the phase modulator constant, as mentioned previously, can only vary over a practical range of 0 to 2.0. If this value is made larger than 2.0, the carrier component of the downlink spectrum passes through zero value, and ground carrier phase lock operation becomes more difficult. A value of 2.0 for D_ϕ can be considered as the maximum value of a "narrow-band" phase modulation system typified by the GRARR system as differentiated from a "wide-band" angle modulation system (phase or frequency modulation).

f_C is set at 2253.0 MHz because that is the frequency of the GRARR transponder output, but it is not a sensitive parameter here. f_a and f_{CF} have been set equal, that is the uplink transmission is translated to the exact center of the transponder IF, but the computer program could accept offset conditions. f_a is set by ground system constraints to be one of 3 subcarrier frequencies, 1.4, 2.4 or 3.2 MHz and has been chosen at 2.4 MHz for the experiment. f_a is not critical for narrow noise bandwidths such as 550 kHz, because the modulating noise at zero frequency is inconsequential. However for a transponder noise bandwidth of 3900 kHz, choice of the 1.4 MHz subcarrier frequency presents a noticeable amount of noise power at zero frequency into the modulator and slightly affects the output spectrum. But in the real, physical, world, it is not possible to have a very wide bandwidth about a small center frequency, so that the value of this type of calculation (performed as a test of the program) is meaningless.

Figure 2a was calculated under the following conditions: $A = \sqrt{2}$, D_ϕ = 1.0, 1.5, and 2.0, N_o varied between 0.0025 to 0.5 watts (see Table II) as a function of input S/N, B_o varied between 1.0 and 0.028025 (for D_ϕ = 1.5 and see Table II), f_B = 219, 418 Hz (noise bandwidth = 550 kHz), f_C = 2253 MHz, f_a = 2.4 MHz, and f_{CF} = 2.4 MHz. The input to the modulator was assumed to be the same

[5] The only alternative to keeping the drive to the modulator a constant would be to adjust the modulator drive as a function of the input signal (input noise stays constant). For low signal to noise ratios at the input, this implies phase locked loop operation and negates the entire utility of the GRARR transponder.

Gaussian shape as the input to the limiter, but the amplitudes of the signal and noise density follow the changes in total output signal to noise as input signal to noise ratio is varied (Condition 1). The statement "limiter degradation of S/W assumed" means that the signal to noise power density, S'/Φ, at the input to the modulator varies between 2 S/W for large S/N, and $\pi/4$ S/W for low S/N. Later it will be shown that this assumption has little effect on the overall result.

The value of the subcarrier power (S_{SC}, sum of upper and lower subcarrier) declines almost linearly with S/N after S/N reaches -10 db, with a phase modulation constant of 1.5 appearing to have a slight advantage over 1.0 or 2.0. The decline in subcarrier power is caused by the noise becoming the modulating signal by suppressing the modulating signal in the limiter. The carrier component S_C, remains relatively constant since the drive to the modulator, whether signal or noise, determines the carrier value at the output of the modulator/transmitter. Small and inconsequential amounts of signal power are present at $f_C \pm mf_a$ where $m = 2, 3, 4 \cdots$, but these powers do not contribute to ground system operation.

Figure 3 was calculated for the same conditions as Figure 2 and presents the signal to noise power density at the carrier $\left[S_C/\Phi_C\ (f = f_C)\right]$, and subcarrier $\left[S_{SC}/2\Phi_{SC}\ (f = f_C \pm f_a)\right]$. On the ground we are interested in the noise power densities at the signal components since these densities can directly affect the phase locked loops in the ground system operation. The signal to noise power density at either subcarrier ($f_C + f_a$ or $f_C - f_a$) is shown as $S_{SC}/2\Phi_{SC}$.

It is apparent in Figure 3 that modulating by the noise does produce a finite but small noise spectral density at the carrier frequency, f_C. If the noise power at the modulator input in the transponder continued to increase as the input S/N decreased, the line showing signal to noise power density at the carrier at large S/N would continue downward as S/N decreased. Remember, however, that the limiter effectively sets the noise power drive to the modulator at a maximum value of 0.5 watts (see Table II). Thus for low signal to noise ratios (below 0 db) the noise power drive to the modulator remains effectively constant and produces a relatively constant signal to noise power density at the carrier frequency. It should be noted here that these small ratios about the carrier frequency will be shown to be unimportant in terms of degradation of ground system operation.

The signal to noise power density at either subcarrier frequency degrades almost linearly with input signal to noise ratio. This is because the signal power into the modulator decreases nearly linearly with decreasing S/N, and below S/N = -20 db the variation of $S_{SC}/2\Phi_{SC}$ is linear.

The dotted line in Figure 3 shows a minimum requirement for either the carrier or subcarrier phase locked loop in the ground system. This is calculated

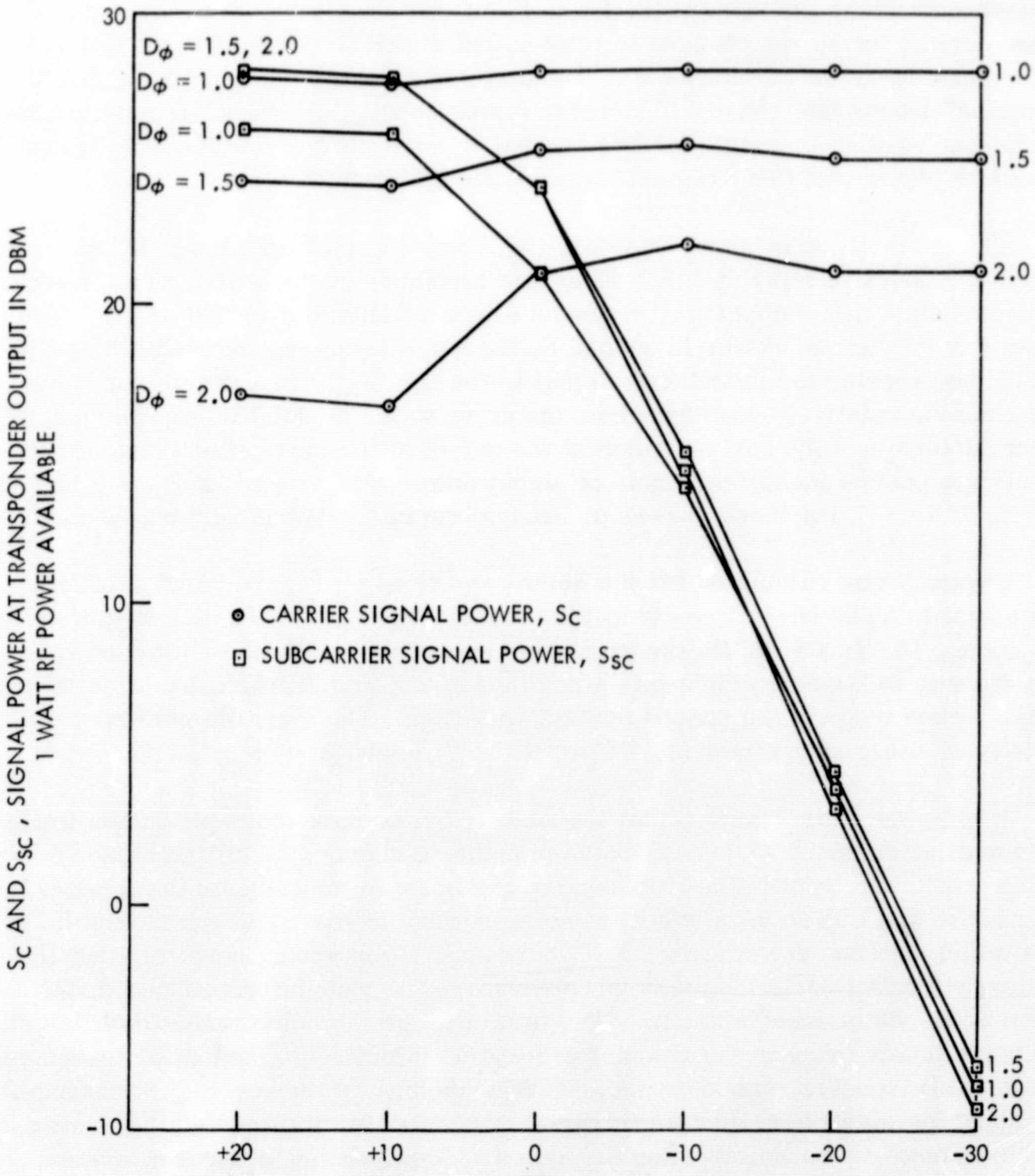

$\frac{S}{N}$ SIGNAL TO NOISE RATIO IN DB AT INPUT TO LIMITER IN TRANSPONDER, 550 kHz TRANSPONDER NOISE BANDWIDTH, LIMITER DEGRADATION OF $\frac{S}{W}$ ASSUMED.

NASA-GSFC-T&DS
Mission & Trajectory Analysis Division
Branch 551 Date 8-69
By Grenchik Plot No. 1191

Figure 2a. Transponder Signal Power Output (550 kHz Noise Bandwidth)

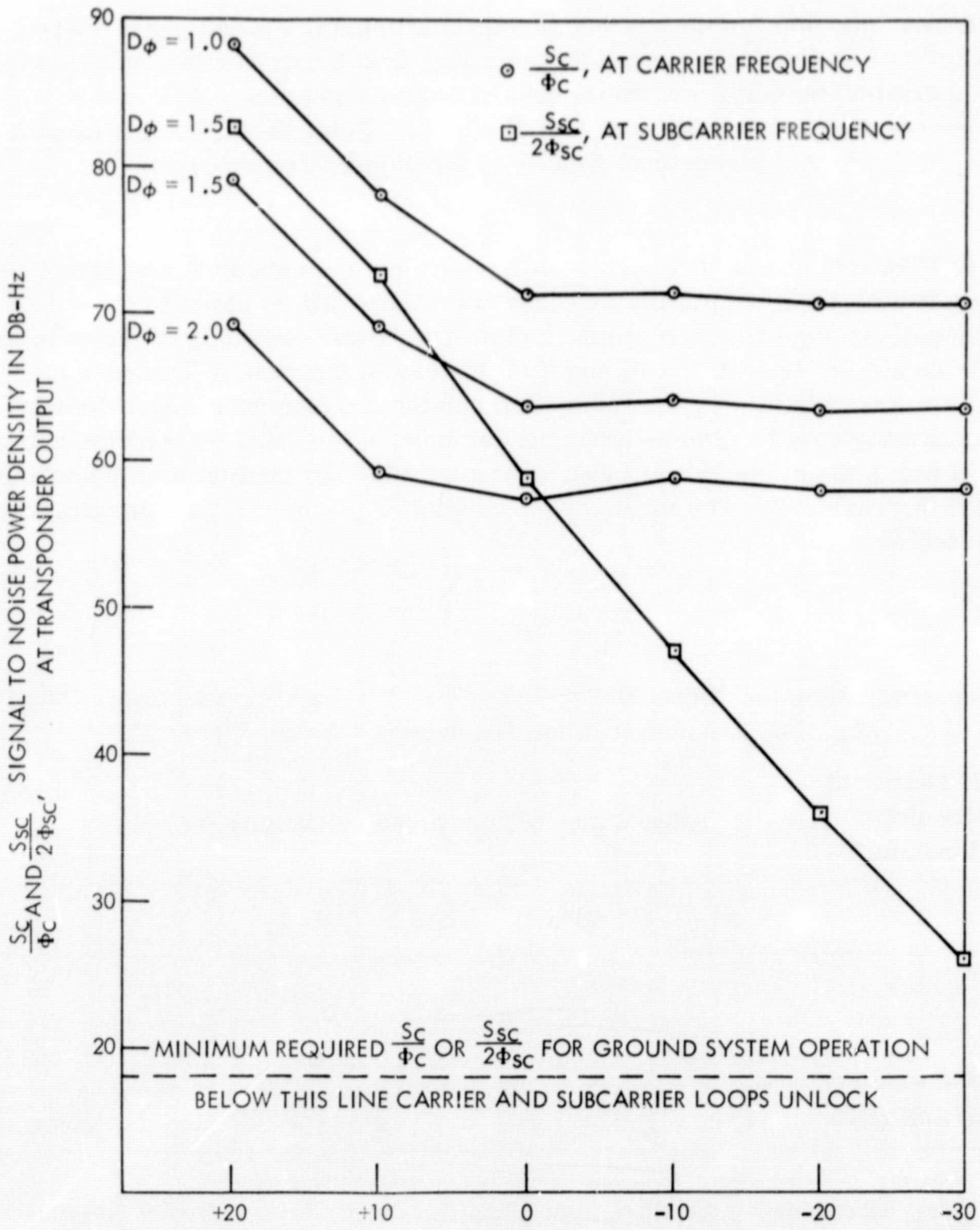

NASA-GSFC-T&DS
Mission & Trajectory Analysis Division
Branch 551 Date 8-69
By Grenchik Plot No. 1192

Figure 3. Transponder Output Signal to Noise Power Density About Signal Components (550 kHz Noise Bandwidth)

as follows: assume for the ground system a minimum 2 sided phase locked loop bandwidth of 20 Hz. At least a 5 db input signal to noise ratio is required for loop operation, so that a minimum required signal to noise power density at the carrier or subcarrier loop input is + 18 db-Hz. Below this line of minimum S_C/Φ_C or $S_{SC}/2\Phi_{SC}$, the ground system is considered inoperative.

In Figure 3, it was difficult to plot values for the subcarrier signal to noise power density for D_ϕ = 1.0 or 2.0 since the values fell so close to D_ϕ = 1.5. Additionally in Figure 2, the graph is cluttered by the crowding of the subcarrier power levels for D_ϕ = 1.0, 1.5, and 2.0. To assist the reader Tables V and VI have been prepared listing the computed values of subcarrier signal to noise power density as a function of transponder input S/N (Table V), and the subcarrier power (sum of upper and lower sideband) also as function of transponder input S/N (Table VI). The modulation constant, D_ϕ, appears as a parameter in these tables.

Table V

Subcarrier Signal to Noise Power Density in DB-Hz at Transponder Output, $S_{SC}/2\Phi_{SC}$, 550 kHz Noise Bandwidth. (From Figure 3)

(Radians/Volt) Modulation Constant, D_ϕ	Output Subcarrier to Noise Density (DB-Hz)					
1.0	81.6	71.5	58.5	47.2	36.3	26.3
1.5	82.9	72.7	58.8	47.0	36.0	26.0
2.0	83.2	72.8	58.6	46.4	35.1	25.1
Input S/N (DB)	+20	+10	0	-10	-20	-30

S/N (DB), Transponder Limiter Input, Limiter Degradation of S/W Assumed.

Figure 4 has been prepared in illustration of the noise spectral density about the subcarrier frequencies (550 kHz transponder noise bandwidth). Only the density about the upper subcarrier, 2255.4 MHz, is shown, but the density at the lower subcarrier, 2250.6 MHz, is identical. The density about the carrier has not been plotted because it is insignificant compared to the subcarrier densities.

Table VI

Subcarrier Signal Power in DBM at Transponder Output, S_{SC} 550 kHz Noise Bandwidth. (From Figure 2)

(Radians/Volt) Modulation Constant, D_ϕ	Output Subcarrier Signal Power (DBM) (Based on One Watt Total Available Power)					
1.0	25.9	25.8	22.5	14.0	3.8	-6.2
1.5	27.9	27.7	24.1	15.2	4.6	-5.4
2.0	28.2	27.8	24.0	14.4	3.2	-6.8
Input S/N (DB)	+20	+10	0	-10	-20	-30

S/N (DB), Transponder Limiter Input, Limiter Degradation of S/W Assumed.

Figure 4 then is a plot of the noise spectral density in dbm-Hz about the upper subcarrier frequency, 2255.4 MHz, for transponder limiter input signal to noise ratios of 100, 10, 1, 0.1, 0.01, and 0.001. The modulation constant, D_ϕ, for this figure was set at 1.5 radians/volt. The total available transmitter power is one watt, and condition 1, limiter degradation of S/W, is assumed. The dotted line shown for reference is the IF bandpass noise spectral density input to the modulator for a S/N of 100. It is shown here to demonstrate the spreading of the tails of the noise power spectral density by the modulation process. Note that for a S/N of 100, the spectral shape of the noise very closely resembles the input noise power spectrum. As S/N decreases, the spectral spreading worsens, until S/N reaches 0.01. At this S/N, the noise power input to the modulator is 0.5 watts and increases no further because of the limiter acting to provide a constant drive to the modulator. Further decreases in S/N do not affect the noise output of the modulator; only the signal S_{SC} continues to decrease with decreasing S/N.

Figure 5 also treats the subcarrier noise power density at the upper subcarrier frequency, but here the S/N into the limiter is held fixed at -30 db (0.001), and D_ϕ is the parameter varied. The dotted line illustrates the IF noise power spectral density at the modulator input, Φ, at S/N = 0.001. For small modulation constants, i. e., $D_\phi = 0.5$, the output spectral density about the subcarrier is very similar to the modulating spectral density, Φ. The spreading of the spectral density increases with increasing modulation constant, D_ϕ, a result which is physically similar to the spreading of the phase modulator output spectrum for deterministic modulations.

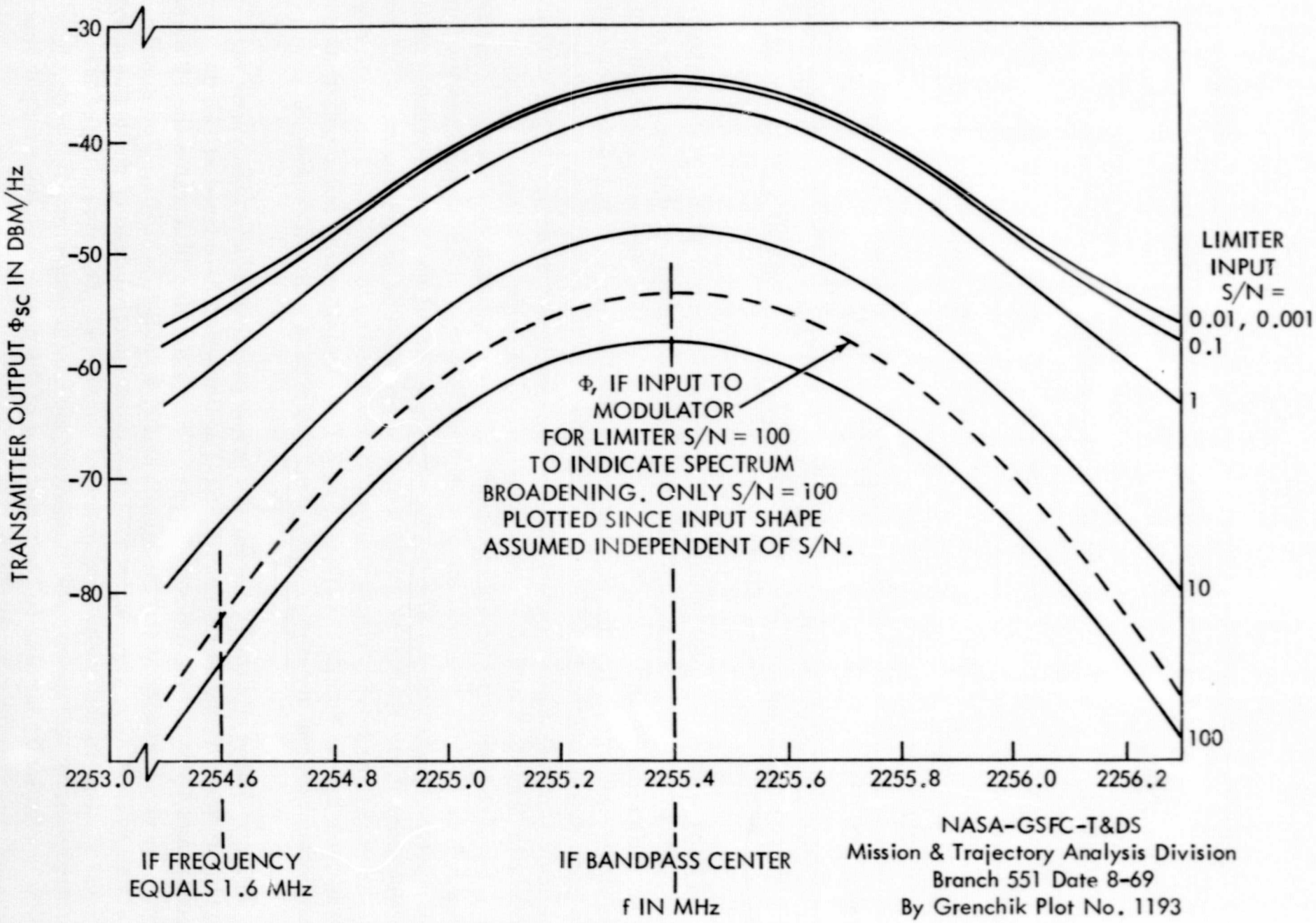

Figure 4. Φ_{SC}, Subcarrier Noise Power Density at Transmitter Output, D_{ϕ} = 1.5, Total Transmitter Power = 1 Watt, Limiter Degradation of S/W Assumed

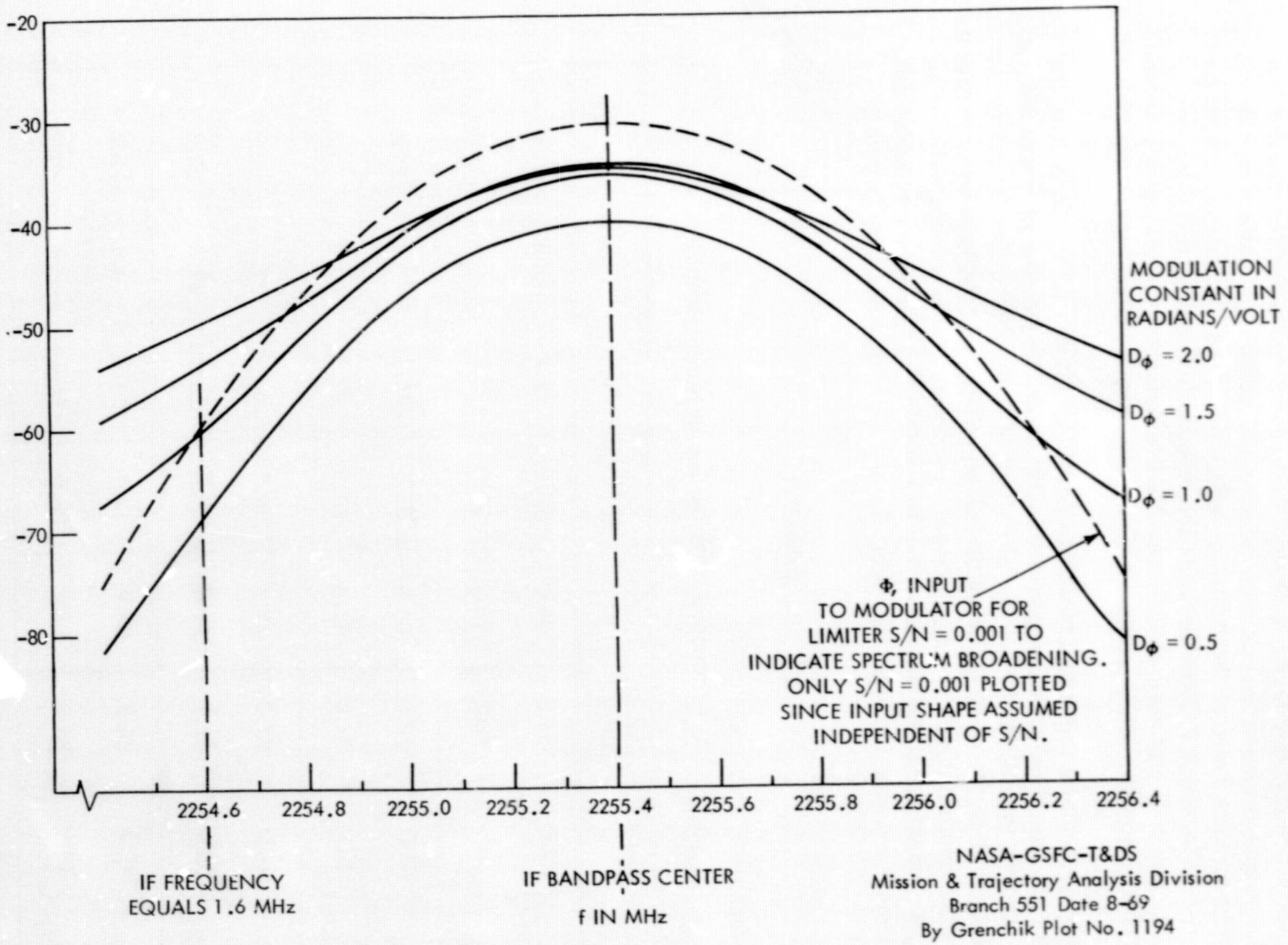

Figure 5. Φ_{SC}, Subcarrier Noise Power Density at Transmitter Output, S/N = -30db, Total Transmitter Power = 1 Watt, Limiter Degradation of S/W Assumed

These preceding figures complete the illustration of the modulator/transmitter output for a transponder noise bandwidth of 550 kHz and under the assumption that the signal to noise power density into the modulator varies as the output signal to noise ratio of the limiter, condition (1). Earlier we had stated that very little differences existed between the results for condition (1), limiter degradation of S/W assumed and the results for condition (2), no limiter degradation of S/W assumed. Here we attempt to justify these statements.

Table VII shows the comparison of Conditions (1) and (2) for $D_\phi = 1.0$. In the top row, the signal to noise power density about the carrier is compared. At an S/N of 100, they differ by 3.0 db, at an S/N of 0.001 they differ by 0.1 db, but a magnitude of S_C/Φ_C of 85 db or 70 db has no effect on ground system operation. The ground system itself (and any ground system) will have a maximally attainable S_C/Φ_C constrained by the imperfections within the system (i. e., instability of reference frequencies) and this limit for the GRARR system is typically 50 db-Hz.

Table VII

Comparison of Modulator/Transmitter Outputs for Conditions (1) and (2), $D_\phi = 1.0$, Transponder Noise Bandwidth = 550 kHz.

Limiter Input S/N		100	10	1	0.1	0.01	0.001
$\frac{S_C}{\Phi_C}$ (DB-Hz)	NLD	85.2	76.0	70.6	70.6	70.8	70.8
	LD	88.2	78.2	71.5	71.6	70.8	70.9
$\frac{S_{SC}}{2\Phi_{SC}}$ (DB-Hz)	NLD	78.5	68.4	57.9	47.4	37.4	27.3
	LD	81.6	71.5	58.5	47.2	36.3	26.3
S_C (DBM)	NLD	27.7	27.7	27.8	27.8	27.8	27.8
	LD	27.7	27.6	28.0	28.0	27.8	27.8
S_{SC} (DBM)	NLD	25.9	25.4	22.4	14.5	4.8	-5.2
	LD	25.9	25.8	22.5	14.0	3.8	-6.2

NLD--Condition (2): No Limiter Degradation of S/W Assumed.

LD--Condition (1): Limiter Degradation of S/W Assumed.

The subcarrier signal to noise power density ($S_{SC}/2\Phi_{SC}$) comparison shows a difference of 3.1 db at S/N = 100, and a difference of 1.0 db at S/N = 0.001. This factor of 3 db for large S/N appears because it was assumed that the signal to noise power density, S/Φ, into the modulator for condition (1) was a factor of 2 poorer than for condition (2). Note that even in condition (2), where the input to the modulator was assumed to be unchanged by any limiter effects, $S_{SC}/2\Phi_{SC}$ decreased 51.2 db for a decrease of S/N of 50 db. This measure is our best comparison of the degradation of the signal to noise power density about the subcarrier by the modulator alone. Here for D_ϕ = 1.0, the degradation is negligible, a 1.2 db departure from linear.

In rows 3 and 4, the carrier and subcarrier powers are compared. The largest difference in carrier power is 0.8 db, and the largest difference in subcarrier power is 1.0 db.

Table VIII is identical to Table VII in all parameters, except that D_ϕ = 1.5. Again, the carrier signal to noise power density has no effect on ground system operation. In the second row, $S_{SC}/2\Phi_{SC}$ differ by 3.1 db at S/N = 100 and 1.0 db at S/N = 0.001. Rows 3 and 4 show maximum differences of 0.5 db and 1.0 db respectively. Note that in row 2 for condition (2), $S_{SC}/2\Phi_{SC}$ decreases by 52.8 db for a S/N decrease of 50 db. This is a slightly larger degradation over the D_ϕ = 1.0 case (2.3 db vs 1.2 db) but still essentially a linear conversion of uplink S/W into downlink subcarrier $S_{SC}/2\Phi_{SC}$.

Table IX follows Table VII and VIII with D_ϕ held at 2.0 radians/volt. Again carrier signal to noise power density is above ground system requirements. The subcarrier signal to noise power density differs by 3.1 db at S/N = 100, and 1.1 db at S/N = 0.001. The carrier powers differ at most 1.3 db, and the subcarrier power by 1.1 db. Over the total range of S/N variation, 50 db, $S_{SC}/2\Phi_{SC}$ varies 3.9 db, compared to 2.8 db for D_ϕ = 1.5, and 1.2 db for D_ϕ = 1.0. Here again it must be stressed that the departure from linear of the output signal to noise power density ($S_{SC}/2\Phi_{SC}$) compared to the input signal to noise S/N for condition (2) is small. However if one considers the output signal to noise POWER ratio about the subcarrier including the broadening of the noise spectrum, it must be concluded that the signal to noise power ratio at the output of the modulator degrades more seriously than the output signal to noise power density just about the subcarrier component. This feature of phase modulation would be analogous to Tausworthe's contention for the limiter, that immediately about the signal, the signal to noise power density essentially is not degraded at the output of the limiter compared to the input, but the broadening of the noise spectral input does effectively degrade the signal to noise ratio at the output.

The preceding paragraphs conclude the presentment of the results for the 550 kHz transponder noise bandwidth. The last remaining features are the results for the 3900 kHz transponder noise bandwidth. The parameters used in the

Table VIII

Comparison of Modulator/Transmitter Outputs for Conditions (1) and (2), D_ϕ = 1.5, Transponder Noise Bandwidth = 550 kHz.

Limiter Input S/N		100	10	1	0.1	0.01	0.001
$\frac{S_C}{\Phi_C}$ (DB-Hz)	NLD	76.2	67.2	62.8	63.[illegible]	63.5	63.6
	LD	79.2	69.1	63.7	64.3	63.6	63.7
$\frac{S_{SC}}{2\Phi_{SC}}$ (DB-Hz)	NLD	79.8	69.5	58.1	47.2	37.0	27.0
	LD	82.9	72.7	58.8	47.0	36.0	26.0
S_C (DBM)	NLD	24.1	24.3	24.9	25.1	25.1	25.1
	LD	24.2	23.9	25.2	25.6	25.1	25.1
S_{SC} (DBM)	NLD	27.9	27.3	23.8	15.4	5.6	-4.4
	LD	27.9	27.7	24.1	15.2	4.6	-5.4

NLD—Condition (2): No Limiter Degradation of S/W Assumed.

LD—Condition (1): Limiter Degradation of S/W Assumed.

calculation are the following: A = $\sqrt{2}$, D_ϕ = 1.0, 1.5, and 2.0, N_o varied between 0.0025 to 0.5 watts (condition 1, see Table II) as a function of input S/N, B_o varied between 1.0 and 0.028025 (for D_ϕ = 1.5 and see Table II), f_B = 1,555,875 Hz (noise bandwidth = 3.9 MHz), f_C = 2253 MHz, f_a = 2.4 MHz, and f_{CF} = 2.4 MHz. The noise input to the modulator was assumed to be the same Gaussian shape as the input to the limiter, but the amplitudes of the signal and noise density follow the changes in total output signal to noise (condition 1). Figure 6 illustrates the signal power output condition for the wider transponder noise bandwidth. Table X should be viewed in conjunction with Figure 6 since crowding of this figure would have resulted if all the information were plotted thereon.

Figure 7 show the signal to noise power densities for the 3,900 kHz transponder noise bandwidth. Table XI presents the additional information which could not be fitted in Figure 7.

Table IX

Comparison of Modulator/Transmitter Outputs for Conditions (1) and (2), D_ϕ = 2.0, Transponder Noise Bandwidth = 550 kHz.

Limiter Input S/N		100	10	1	0.1	0.01	0.001
$\frac{S_C}{\Phi_C}$ (DB-Hz)	NLD	66.2	58.1	56.4	57.7	58.0	58.0
	LD	69.2	59.2	57.3	58.9	58.0	58.1
$\frac{S_{SC}}{2\Phi_{SC}}$ (DB-Hz)	NLD	80.1	69.6	57.7	46.4	36.2	26.2
	LD	83.2	72.8	58.6	46.4	35.1	25.1
S_C (DBM)	NLD	16.9	17.9	20.5	21.2	21.2	21.2
	LD	17.0	16.6	21.2	22.1	21.2	21.3
S_{SC} (DBM)	NLD	28.1	27.5	23.3	14.2	4.3	-5.7
	LD	28.2	27.8	24.0	14.4	3.2	-6.8

NLD—Condition (2): No Limiter Degradation of S/W Assumed.

LD—Condition (1): Limiter Degradation of S/W Assumed.

Finally, Table XII shows the comparison of modulator output for conditions (1) and (2) with the phase modulator constant, D_ϕ, held at 1.5 radians/volt. It was deemed unnecessary to present the comparisons for D_ϕ = 1.0 and 2.0.

With these preceding results covering all applicable conditions of modulation constant, noise bandwidth, and signal to noise input ratio, we are now in a position to calculate the effect of the weak uplink conditions in the ATS-F/NIMBUS-E tracking data relay experiment.

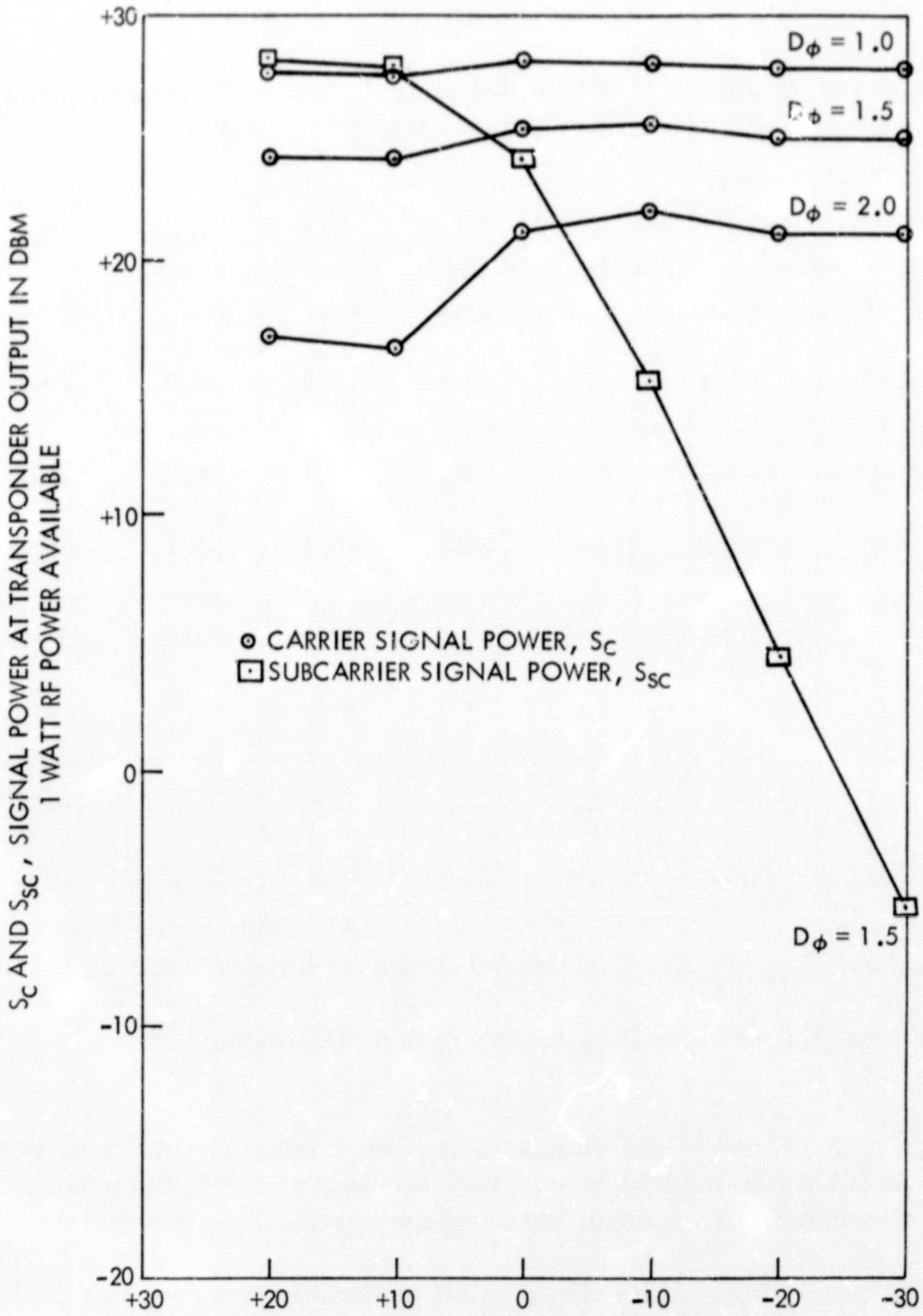

NASA-GSFC-T° DS
Mission & Trajectory Analysis Division
Branch 551 Date 8-69
By Grenchik Plot No. 1195

Figure 6. Transponder Signal Power Output (3900 kHz Noise Bandwidth)

Table X

Subcarrier Signal Power in DBM at Transponder Output, S_{SC}, 3900 kHz Noise Bandwidth (From Figure 6).

(Radians/Volt) Modulation Constant, D_ϕ	Output Subcarrier Signal Power (DBM) (Based on One Watt Total Available Power)					
1.0	25.9	25.8	22.5	14.1	3.8	-6.2
1.5	27.9	27.7	24.1	15.2	4.6	-5.4
2.0	28.2	27.8	24.0	14.4	3.2	-6.7
Input S/N (DB)	+20	+10	0	-10	-20	-30

S/N (DB), Transponder Limiter Input, Limiter Degradation of S/W Assumed.

Table XI

Subcarrier Signal to Noise Power Density in DB-Hz at Transponder Output, $S_{SC}/2\Phi_{SC}$, 3900 kHz Noise Bandwidth (From Figure 7).

(Radians/Volt) Modulation Constant, D_ϕ	Output Subcarrier to Noise Density (DB-Hz)					
1.0	88.9	78.8	66.2	55.1	44.1	34.1
1.5	88.5	78.4	65.6	54.3	43.1	33.1
2.0	87.2	77.0	64.5	52.8	41.4	31.4
Input S/N (DB)	+20	+10	0	-10	-20	-30

S/N (DB), Transponder Limiter Input, Limiter Degradation of S/W Assumed.

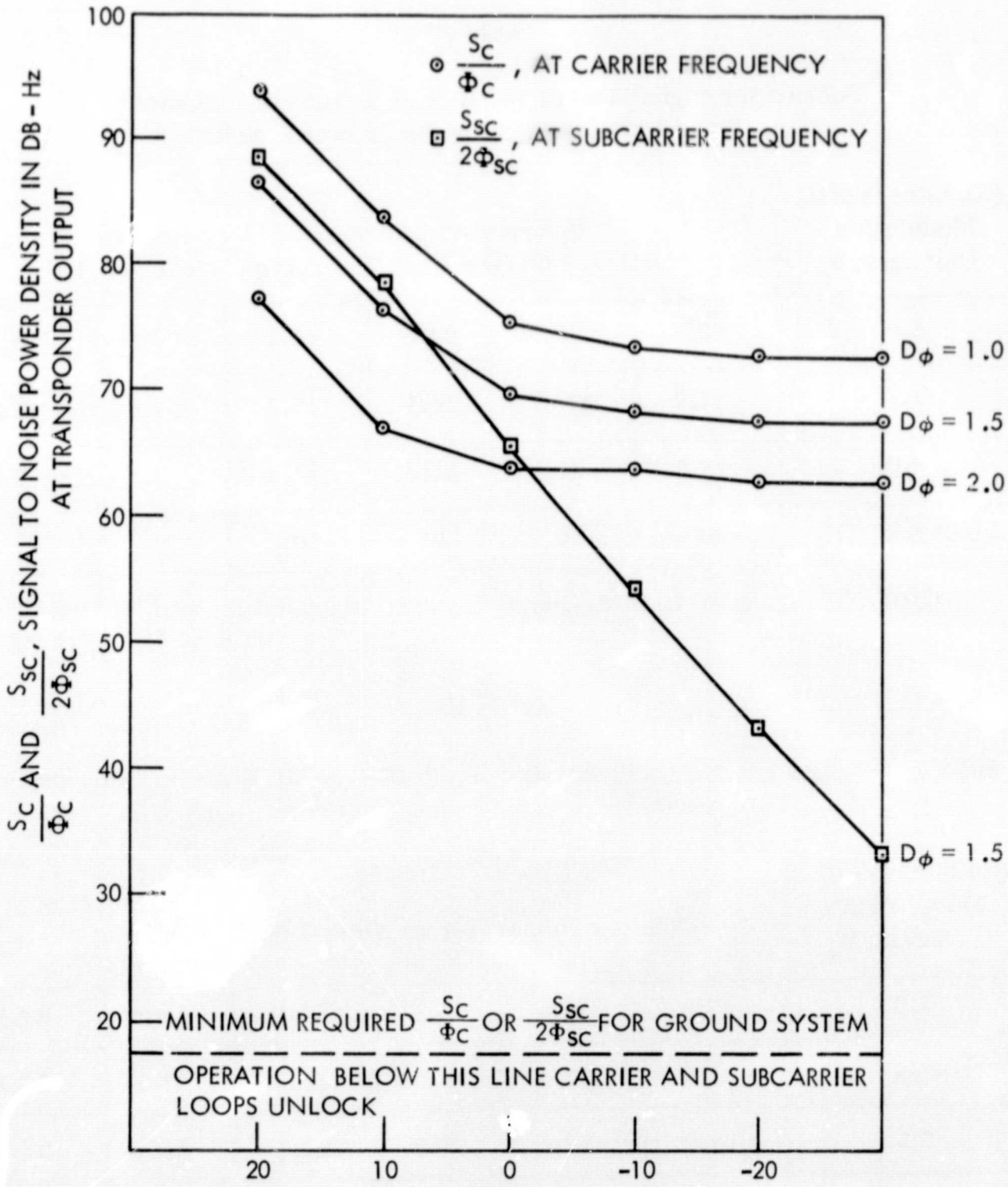

NASA-GSFC-T&DS
Mission & Trajectory Analysis Division
Branch 1196 Date 8-69
By Grenchik Plot No. 1196

Figure 7. Transponder Output Signal to Noise Power Density About Signal Components (3900 kHz Noise Bandwidth)

Table XII

Comparison of Modulator/Transmitter Outputs for Conditions (1) and (2), D_ϕ = 1.5, Transponder Noise Bandwidth = 3900 kHz.

Limiter Input S/N		100	10	1	0.1	0.01	0.001
$\frac{S_C}{\Phi_C}$ (DB-Hz)	NLD	82.4	74.2	68.7	67.6	67.5	67.5
	LD	86.4	76.4	69.6	68.4	67.6	67.6
$\frac{S_{SC}}{2\Phi_{SC}}$ (DB-Hz)	NLD	85.5	75.4	64.8	54.3	44.2	34.2
	LD	88.5	78.4	65.6	54.3	43.1	33.1
S_C (DBM)	NLD	24.1	24.3	24.9	25.1	25.1	25.1
	LD	24.2	23.9	25.2	25.6	25.1	25.1
S_{SC} (DBM)	NLD	27.9	27.3	23.8	15.4	5.6	-4.4
	LD	27.9	27.7	24.1	15.2	4.6	-5.4

NLD: Condition (2): No Limiter Degradation of S/W Assumed.

LD: Condition (1): Limiter Degradation of S/W Assumed.

6. APPLICATION OF MODULATION RESULTS TO ATS-F/NIMBUS-E TRACKING EXPERIMENT

Reference 10 describes in detail the parameter of the ATS-F/NIMBUS-E tracking links. It is the intent here to use the parameters of that reference, and the theory and result of sections 4 and 5 herein, to show the degradation in the range rate measurement in the ground tracking system. Figure 8 presents a functional block diagram which illustrates the nominal link parameter. The value of the parameters are taken specifically from section 9.5, Tables 9.5-1B, 9.5-2B, 9.5-3B, and 9.5-4B of reference 10. For example between ① and ② in Figure 8, the uplink parameters to ATS-F total to a value of -134.8 db. This total includes ground transmit antenna gain, miscellaneous transmit losses, free space loss, ATS-F receive antenna gain, ATS-F antenna polarization loss, and miscellaneous receive losses on the ATS-F spacecraft.

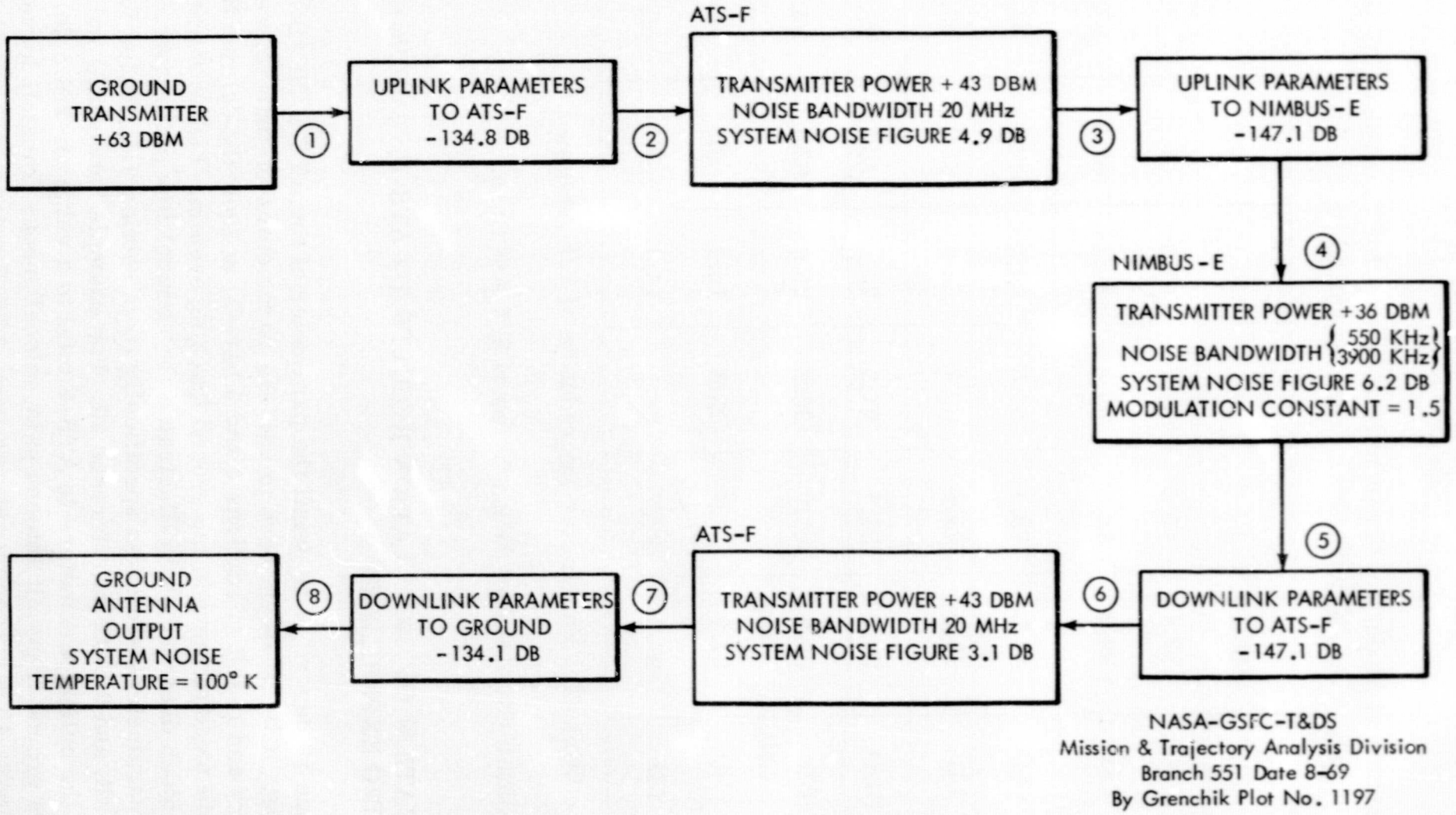

Figure 8. Functional Block Diagram of Ground/ATS-F/NIMBUS-E Link (Nominal Conditions)

Table XIII has a sample calculation for the resultant signal to noise power density at the ground for the nominal conditions shown in Figure 8, and for the conditions of $D_\phi = 1.5$ and a transponder noise bandwidth of 550 kHz. Definitions in Table XIII are as follows:

S_{IN} —signal power input in dbm

N_{IN} —noise power input in dbm

N_{INT} —internally generated noise power of following block, referred to input of block, in dbm

S_{INC} —carrier signal power input in dbm

S_{INSC} —subcarrier signal power input, sum of upper and lower spectral components, in dbm

N_{INC} —input noise power about the carrier in dbm

N_{INSC} —input noise power about the subcarrier in dbm

The values for the carrier and subcarrier power levels at point ⑤, GRARR transponder phase modulator/transmitter output, were taken from Figure 2 (condition 1).

At point ⑥ in Table XIII, the input noise powers about the carrier and subcarrier (N_{INC} and N_{INSC}), generated in the GRARR transponder and attenuated in downlink ⑤ → ⑥, are negligible compared to the internally generated noise within the ATS-F transponder. Thus from block ⑥ on, the only important noise component is the ATS-F transponder noise relayed to the ground system. Note that the ATS-F transponder noise at point ⑧, N_{IN}, even after attenuation in link ⑦ → ⑧, is still dominant compared to the internal noise of the ground system, N_{INT}. The ATS-F transponder noise, in essence, sets the value of Φ_G, the noise power density in the ground system.

One simplification made in the calculations of Table XIII should be explained. At the ATS-F transponder in either the uplink or the downlink, the signal and noise power relayed up or down were calculated on the basis of maintaining the input signal and noise ratios at the output of the transponder, and holding the total output power at +43 dbm. This assumes a linear limiter or AGC system in the ATS-F transponder on both the uplink and the downlink.

Similar calculations to those in Table XIII were made for the transmit/receive antenna on NIMBUS-E at other values than 16 db/14 db. For example

Table XIII

Sample Calculation of Ground Signal to Noise Power Density for ATS-F/ NIMBUS-E Links, Nominal Conditions, 550 kHz Transponder Noise Bandwidth, D_ϕ = 1.5.

(DBM)	①	②	③	④
S_{IN}	+63	-71.8	43.0	-104.1
N_{IN}	-	-235.8 (20 MHz)	18.7 (20 MHz)	-128.4 (20 MHz)
N_{INT}	-101 (20 MHz)	-96.1 (20 MHz)	-101 (20 MHz)	-110.4 (550 kHz)
$N_{IN} + N_{INT}$	-101 (20 MHz)	-96.1 (20 MHz)	18.7 (20 MHz)	-110.4 (550 kHz)

(DBM)	⑤	⑥
S_{INC}	30.5	-116.6
S_{INSC}	32.2	-114.9
N_{INC}	20.9 (550 kHz)	-126.2 (550 kHz)
N_{INSC}	22.6 (1100 kHz)	-124.5 (1100 kHz)
N_{INT}	-101 (20 MHz)	-97.9 (20 MHz) -113.5 (550 kHz)
$N_{INC} + N_{INT}$	20.9 (550 kHz)	-113.5 (550 kHz)
$N_{INSC} + N_{INT}$	22.6 (1100 kHz)	-110.5 (1100 kHz)

(DBM)	⑦	⑧
S_{INC}	24.2	-109.9
S_{INSC}	25.9	-108.2
N_{IN}	42.9 (20 MHz)	-91.2 (20 MHz)
N_{INT}	-101 (20 MHz)	-105.6 (20 MHz)
$N_{IN} + N_{INT}$	42.9 (20 MHz)	-91.2 (20 MHz)

S_{GC}/Φ_{GC} = -109.9 - (-91.2 -73.0) = 54.3 db-Hz

$S_{GSC}/2\Phi_{GSC}$ = -108.2 - (-91.2 - 73.0) = 56.0 db-Hz.[6]

[6]Since the ATS-F transponder noise about the upper subcarrier frequency is not correlated with the ATS-F transponder noise about the lower subcarrier frequency, the ground system demodulation process which coherently sums the upper and lower subcarriers, also non-coherently sums the ATS-F transponder noise about these signal components. In effect a 3 db improvement is obtained and the resultant subcarrier signal to noise power density in the ground system is equal to the sum of the upper and lower signal subcarrier power, divided by the noise power density. This is in contrast to Figures 3 and 7, and Tables V, VII, VIII, IX, XI, and XII, wherein the GRARR transponder noise at the upper and lower subcarrier frequencies is correlated, and $S_{SC}/2\Phi_{SC}$ is the value for the subcarrier signal to noise power density.

with a 2 db/0 db antenna on Nimbus-E, the blocks between points ③ and ④, and between ⑤ and ⑥ have attenuation of 161.1 db compared to nominal conditions of 147.1 db and the signal to noise ratio at the input to the GRARR transponder decreases 14 db. Other values of transmit/receive antenna gain were assumed and calculations were made for the effect in the ground system operation. Figure 9 presents the ground signal to noise power densities at the carrier and subcarrier frequencies for the case of a 550 kHz transponder noise bandwidth, and under condition 1. Condition 2 results would be for all practical purposes, identical to Figure 9. In addition, modulation constants setting between 1.0 and 2.0 also would produce insignificant changes (at low S/N) in Figure 9, which was calculated for $D_\phi = 1.5$.

It must be stressed that Figure 9 was computed by varying both the uplink and downlink Nimbus antenna gain (one antenna) so that the uplink signal to noise ratio at the GRARR transponder decreased in proportion to the decrease in Nimbus-E receive antenna gain. The downlink carrier and subcarrier signal power decreased in proportion to the decrease in Nimbus-E downlink antenna gain. Thus, below 0 db in Figure 9, the carrier degrades proportional to the decrease in transmit antenna gain (carrier output remains constant, whether modulation is signal or noise), and the subcarrier degrades proportional to the square of the decrease in antenna gain (less subcarrier power out of modulator because of reduced uplink power, and less downlink subcarrier power available at ground because of additional attentuation in downlink).

Figure 10 presents the results for a transponder noise bandwidth of 3900 kHz with all other parameters remaining the same as in Figure 9. Note that in Figure 10 at nominal conditions (receive antenna gain = 14 db), the subcarrier signal to noise power density is already near the value of 50 db-Hz, the desired value for the tracking relay experiment. The reasons for the poorer performance of the wider noise bandwidth case are twofold: (1) under the nominal conditions, N_o, the noise power into the modulator is larger and hence the term $\exp\left[-D_\phi^2 N_o\right]$ which multiplies the signal component in Equation (76) is smaller for the larger noise bandwidth (larger N_o). This is equivalent to less subcarrier signal power available at the ground.

(2) The argument of the Bessel function in Equation (76) is $B_o D_\phi$, and B_o depends upon N_o. As N_o increases, B_o decreases. This is readily apparent in Tables II and III. The noise power transmitted from Nimbus-E and described by $\Phi_x(f)_{n\neq 0}$ is negligible after attenuation in the downlink compared to the internal noise of the ATS-F transponder, so that it does not enter directly into the link degradation.

In conjunction with the results of Figures 9 and 10, one further comment is required. Recall that early in the discussion it was stated that the signal uplink was unmodulated but that investigation should be made into the case of a

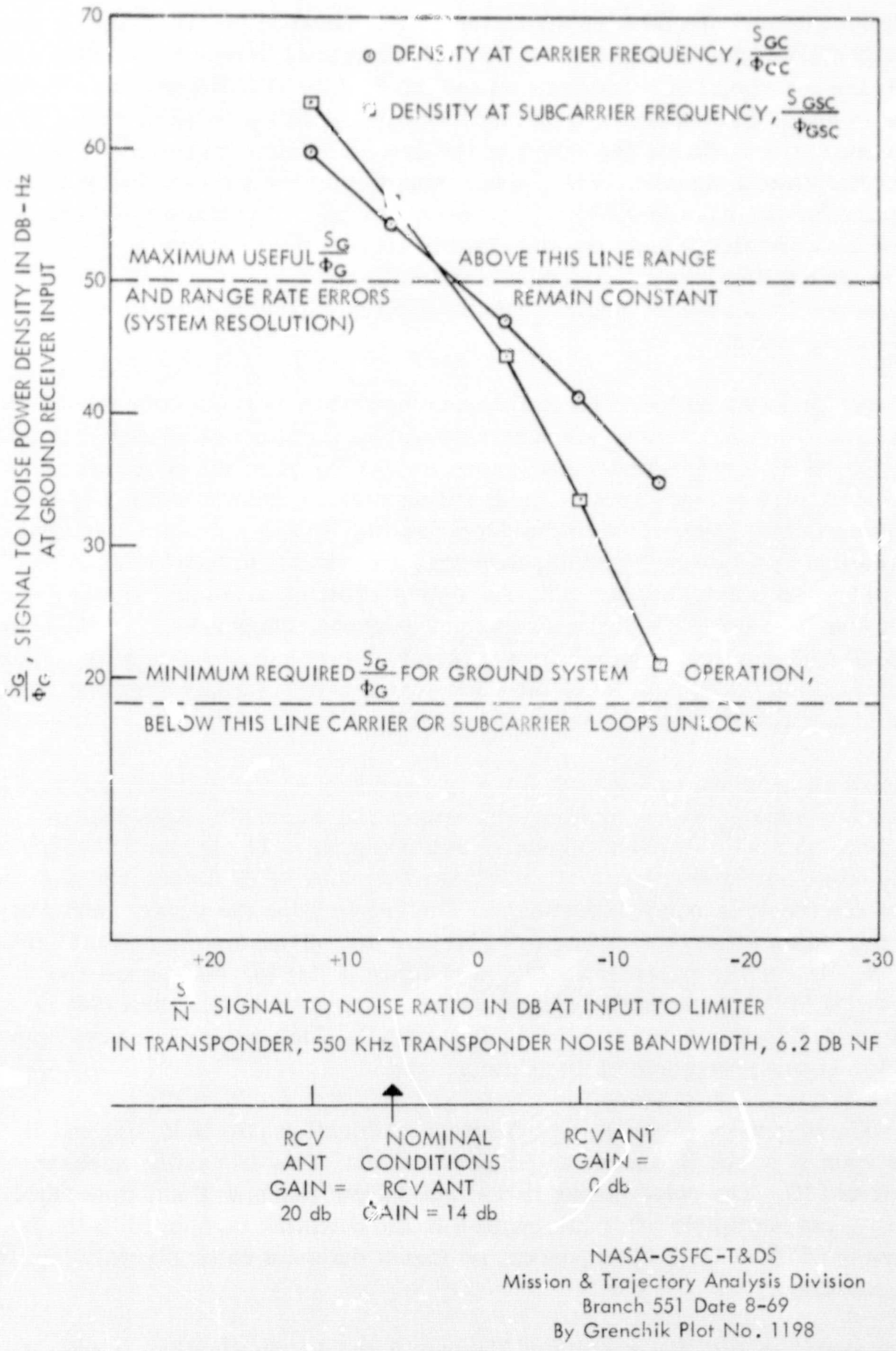

Figure 9. Ground System Signal to Noise Power Density Ratio, Transponder Noise Bandwidth = 550 kHz

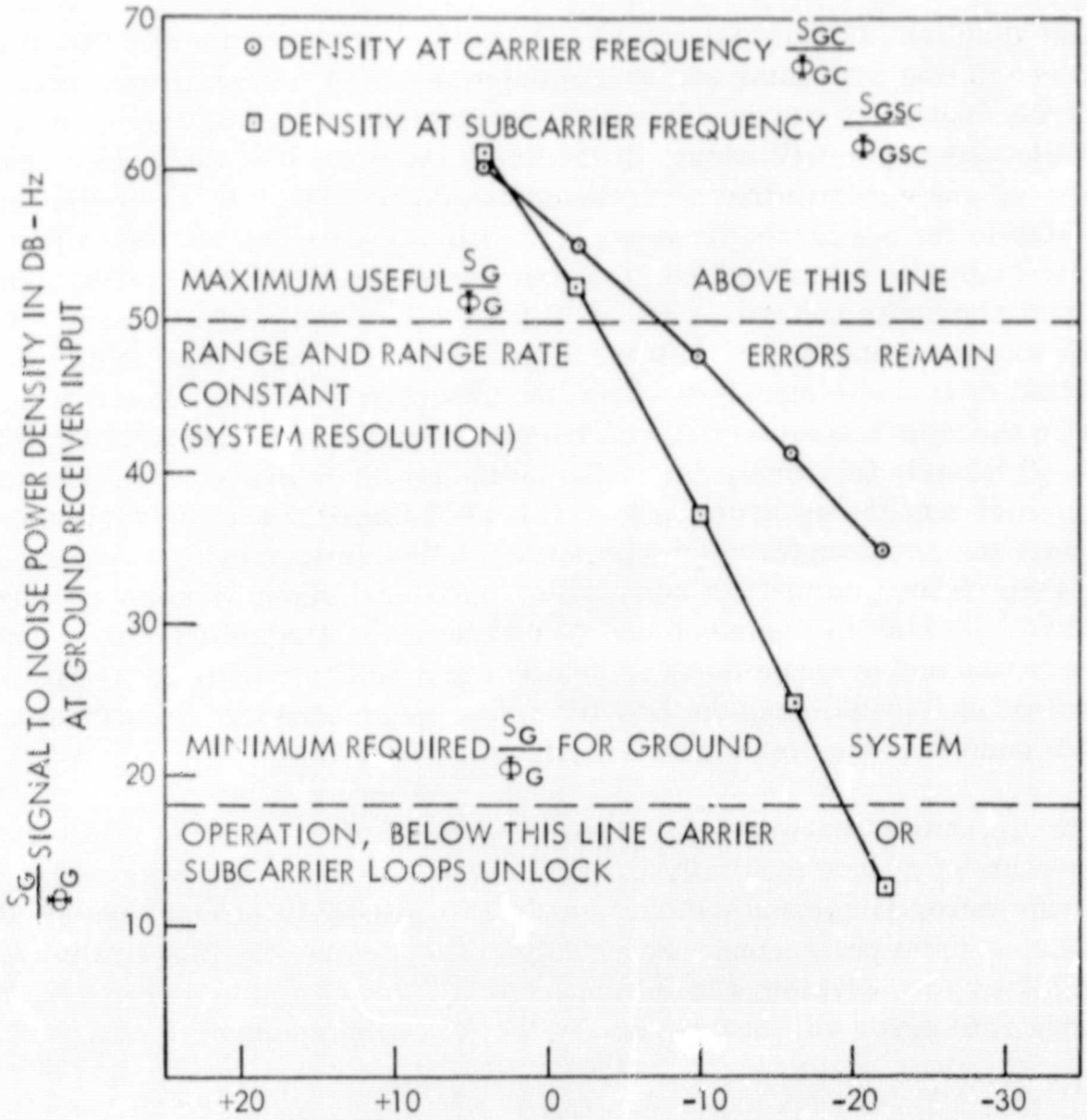

NASA-GSFC-T&DS
Mission & Trajectory Analysis Division
Branch 551 Date 8-69
By Grenchik Plot No. 1199

Figure 10. Ground System Signal to Noise Power Density Ratio, Transponder Noise Bandwidth = 3900 kHz

modulated uplink. This is intended by the author, but from the results of low index modulating with noise and unmodulated signal, it is anticipated that a similar almost linear transfer of the uplink and noise spectrum to the downlink subcarrier spectrum will occur. If the uplink is modulated, the signal spectrum rather than one spectral line as in the unmodulated case, will be almost linearly translated to the subcarrier frequencies. If this proves so, and the author strongly feels this to be the case, the line representing the subcarrier signal to noise power density in Figures 9 and 10 will be lowered a constant value for all S/N into the transponder limiter. For example, if the ground signal is phase modulated by a single tone of 100 kHz, the ground modulation index is 1.06, the power in the uplink carrier is 2.6 db below the case of the unmodulated uplink signal. Obviously the remainder of the uplink power is available in the modulation portion of the spectrum. Now, if it is assumed that this signal spectrum, along with the transponder noise spectrum are the subcarrier spectral components, then we must adjust the subcarrier signal and signal to noise power density downward by 2.6 db in Figures 9 and 10 for the modulated uplink case. This conjecture by the author remains to be verified, but hopefully it is manifest to the reader that one should keep the GRARR transponder bandwidth as narrow as possible under weak uplink signal conditions.

Finally, some further explanation of the value of 50 db-Hz is required here. At this value of ground input signal to noise power density the value of the random range rate error is approximately 1 cm/sec for a GRARR ground system data rate of 1 measurement per second. For a value of 60 db-Hz, the range rate error still remains 1 cm/sec (system resolution). For a value of 40 db-Hz for S_{GSC}/Φ_{GSC}, the range rate error will change, and in the following manner:

$$\sigma_{\dot{R}} \propto \left(\frac{\Phi_{GSC}}{S_{GSC}}\right)^{1/2} .$$

If the Nimbus-E antenna gain (up and down) were decreased 10 db so that the value of S_{GSC}/Φ_{GSC} drops from 50 db-Hz to 30 db-Hz, the ground range rate error would increase by a factor of 10 or from a 1 cm/sec to a 0.1 m/sec range rate random error. This perhaps is the best illustration of the necessity for avoiding conditions which bring the ground signal to noise density in a tracking relay situation below the value for system resolution.

7. CONCLUSIONS

The mathematical analysis of signal and noise phase modulation has shown that an almost linear translation of the IF spectrum to the RF spectrum occurs

for low modulation index. The nonlinearity of the translation occurs in the tails of the spectral density, but about the signal components, the signal to noise power density is, for all practical purposes, retained in the modulation process. This simplifies considerably the calculation of signal and noise power densities throughout the tracking data relay multiple link.

It has been emphasized that both uplink and downlink must be investigated for the tracking data relay links. In the preceding sections, it was shown how weak uplink signal conditions at the input to the target transponder directly affected the downlink conditions. Specifically for the ATS-F/NIMBUS-E tracking experiment, to avoid undesirable ground system operation (nominal operation below system resolution), it is recommended that:

(1) Use the minimum transponder bandwidth consistent with the ranging accuracy requirements. The author's recommended value is 550 kHz, implying that the maximum uplink modulation should be no greater than 100 kHz.

(2) Plan for the nominal values of the Nimbus-E antenna gain, 16 db transmit and 14 db receive, since they are adequate for acceptable ground system operation. The author stresses that any significant decreases in these gain values will seriously degrade ground system operation.

(3) Use a modulation index of 1.5 radians since it has slight advantages over lower and higher values.

(4) It is not advantageous to procure extremely low ground system noise temperatures, because the ATS-F transponder noise sets the noise power level in the ground system. When considering the tracking relay experiment alone, the cost incurred in extreme reduction of the ground system temperature is wasted.

REFERENCES

1. Rowe, H. E., Signals and Noise in Communication Systems. D. Van Nostrand Company, Inc., 1965.

2. Middleton, David, An Introduction to Statistical Communication Theory, McGraw-Hill Book Company, Inc., 1960.

3. Schwartz, Mischa; Bennett, William R.; and Stein, Seymour, Communication Systems and Techniques, McGraw-Hill Book Company, 1966.

4. Lee, Y. W., Statistical Theory of Communication, John Wiley and Sons, Inc., 1960.

5. Bennett, W. R., "Methods of Solving Noise Problems", Proceedings of the IRE, May 1956, pgs. 609-638.

6. Davenport, W. B. Jr., "Signal-to-Noise Ratios in Band-Pass Limiters", Journal of Applied Physics, Volume 24, Number 6, June 1953, pgs. 720-727.

7. Kronmiller, G. C. Jr., and Baghdady, E. J., "The Goddard Range and Range Rate Tracking System: Concept, Design, and Performance", Goddard Space Flight Center, X-531-65-403, October 1965.

8. "GRARR Power Spectrum, Threshold Analysis, and Spectrum Diagrams", Goddard Space Flight Center, X-530-67-160, April 1967.

9. Goddard Space Flight Center Specification, "Goddard Range and Range Rate System, S-Band Transponder", S-530-P-2, January 1967.

10. Goddard Space Flight Center Document, "ATS-F/NIMBUS-E Data Relay Experiment Technical Summary", GSFC Number DR 1-0000, Revision B, February 3, 1969.

11. Springett, J. C., "A Note on Signal-to-Noise and Signal-to-Noise Spectral Density Ratios at the Output of a Filter-Limiter Combination", JPL Space Programs Summary, No. 37-36, Vol. IV, December 1965, pgs. 241-244.

12. Abramson, Norman, "Bandwidth and Spectra of Phase-and-Frequency Modulated Waves" IEEE Transactions on Communication Systems, December 1963, pgs. 407-414.

13. Tausworthe, R. C., "Information Processing: Limiters in Phase-Locked Loops: A Correction to Previous Theory", JPL Space Programs Summary 37-54, Vol. III, December 1968.

APPENDIX A

CONVERGENCE OF SERIES, $W_x(f)_{n\neq 0}$

Equation (77) in the text presented the equation for the noise power spectral density:

$$W_x(f)_{n\neq 0} = \frac{A^2}{\sqrt{\pi}\, 2^{7/2} f_B} \exp\left(-D_\phi^2 N_o\right) \sum_{m=0}^{6} \sum_{n=1}^{\infty} \sum_{k=0}^{[n/2]} \sum_{p=1}^{8} \frac{\epsilon_m J_m^2\left(B_o D_\phi\right) D_\phi^{2n} N_o^n}{\sqrt{n}\, 2^n\, k!\,(n-k)!}$$

$$\epsilon_{n-2k} \exp\left(\frac{-\gamma_p^2}{8n\pi^2 f_B^2}\right). \quad \text{(A-1)}$$

Here we wish to examine this series convergence. Let

$$K = \frac{A^2}{\sqrt{\pi}\, 2^{7/2} f_B} \exp\left(-D_\phi^2 N_o\right) . \quad \text{(A-2)}$$

Also the following terms have their maximum values as follows:

$$\left(\epsilon_m\right)_{max} = 2 \quad \text{(A-3)}$$

$$\left[J_m^2\left(B_o D_\phi\right)\right]_{max} = 1 \quad \text{(A-4)}$$

$$\left(\epsilon_{n-2k}\right)_{max} = 2 \quad \text{(A-5)}$$

$$\left[\exp\left(\frac{-\gamma_p^2}{8n\pi^2 f_B^2}\right)\right]_{max} = 1 . \quad \text{(A-6)}$$

Then $W_x(f)_{n\neq 0}$ must always be equal to or less than:

$$W_x(f)_{n\neq 0} \leq (K)(2)(7)(2)(8) \sum_{n=1}^{\infty} \sum_{k=0}^{[n/2]} \frac{D_\phi^{2n} N_o^n}{\sqrt{n}\, 2^n\, k!(n-k)!} \qquad \text{(A-7)}$$

$$W_x(f)_{n\neq 0} \leq 224\,K \sum_{n=1}^{\infty} \sum_{k=0}^{[n/2]} \frac{D_\phi^{2n} N_o^n}{\sqrt{n}\, 2^n\, k!(n-k)!} \qquad \text{(A-8)}$$

Here we examine a few terms of the double summation:

$$n = 1: \quad \frac{D_\phi^2 N_o}{2} \qquad \text{(A-9)}$$

$$n = 2: \quad \sum_{k=0}^{1} \frac{D_\phi^4 N_o^2}{\sqrt{2}\, 2^2\, k!(2-k)!} = \frac{(D_\phi^2 N_o)^2}{2^2 \sqrt{2}} \left[\frac{1}{2!} + \frac{1}{1!\,1!}\right] \qquad \text{(A-10)}$$

$$n = 3: \quad \sum_{k=0}^{1} \frac{D_\phi^6 N_o^3}{\sqrt{3}\, 2^3\, k!(3-k)!} = \frac{(D_\phi^2 N_o)^3}{2^3 \sqrt{3}} \left[\frac{1}{3!} + \frac{1}{1!\,2!}\right] \qquad \text{(A-11)}$$

$$n = 4: \quad \sum_{k=0}^{2} \frac{D_\phi^8 N_o^4}{\sqrt{4}\, 2^4\, k!(4-k)!} = \frac{(D_\phi^2 N_o)^4}{2^4 \sqrt{4}} \left[\frac{1}{4!} + \frac{1}{3!} + \frac{1}{2!\,2!}\right] \qquad \text{(A-12)}$$

$$n = 5: \quad \sum_{k=0}^{2} \frac{D_\phi^{10} N_o^5}{\sqrt{5}\, 2^5\, k!(5-k)!} = \frac{(D_\phi^2 N_o)^5}{2^5 \sqrt{5}} \left[\frac{1}{5!} + \frac{1}{4!} + \frac{1}{2!\,3!}\right] \qquad \text{(A-13)}$$

$$n = 6: \quad \sum_{k=0}^{3} \frac{D_\phi^{12} N_o^6}{\sqrt{6}\, 2^6\, k!(6-k)!} = \frac{(D_\phi^2 N_o)^6}{2^6 \sqrt{6}} \left[\frac{1}{6!} + \frac{1}{5!} + \frac{1}{2!\,4!} + \frac{1}{3!\,3!}\right] \qquad \text{(A-14)}$$

The last term in each series is the largest term so that:

$$\sum_{n=1}^{\infty} \sum_{k=0}^{[n/2]} \frac{D_\phi^{2n} N_o^n}{\sqrt{n}\, 2^n\, k!\, n-k!} < \sum_{n=1}^{\infty} \frac{\left(D_\phi^2 N_o\right)^n}{2^n \sqrt{n}} \left[\frac{n}{2} + 1\right] \frac{1}{\Gamma\left(\frac{n}{2}+1\right) \Gamma\left(\frac{n+1}{2}\right)} \qquad \text{(A-15)}$$

where $\Gamma(x)$ is the gamma or generalized factorial function with argument (x). To the infinite summation on the right of Equation A-15, we apply the ratio test to determine the region of convergence:

$$\left| \frac{\frac{\left(D_\phi^2 N_o\right)^{n+1}}{2^{n+1}\sqrt{n+1}} \left(\frac{n+1}{2}+1\right) \frac{1}{\Gamma\left(\frac{n+1}{2}+1\right)\Gamma\left(\frac{n+1+1}{2}\right)}}{\frac{\left(D_\phi^2 N_o\right)^n}{2^n \sqrt{n}} \left(\frac{n}{2}+1\right) \frac{1}{\Gamma\left(\frac{n}{2}+1\right)\Gamma\left(\frac{n+1}{2}\right)}} \right| = \left| \frac{D_\phi^2 N_o \sqrt{n}}{2\sqrt{n+1}} \frac{\left(\frac{n+3}{2}\right)\Gamma\left(\frac{n+1}{2}\right)}{\left(\frac{n+2}{2}\right)\Gamma\left(\frac{n+3}{2}\right)} \right| . \qquad \text{(A-16)}$$

From the gamma function fundamental relation:

$$\Gamma(x+1) = x\Gamma(x) \qquad x > 0 \qquad \text{(A-17)}$$

$$\Gamma\left(\frac{n+3}{2}\right) = \Gamma\left(\frac{n+1}{2}+1\right) = \frac{n+1}{2}\Gamma\left(\frac{n+1}{2}\right) . \qquad \text{(A-18)}$$

Equation (A-16) simplifies to:

$$\left| \frac{D_\phi^2 N_o \sqrt{n}}{2\sqrt{n+1}} \frac{\left(\frac{n+3}{2}\right)}{\left(\frac{n+2}{2}\right)\left(\frac{n+1}{2}\right)} \right| = \left| \frac{D_\phi^2 N_o \sqrt{n}\,(n+3)}{\sqrt{n+1}\,(n+2)\,(n+1)} \right| . \qquad \text{(A-19)}$$

For large n the right side of Equation A-19 approaches:

$$\left| \frac{D_\phi^2 N_o}{n} \right| \qquad \text{(A-20)}$$

and in the limit as n approaches infinity, (A-20) vanishes. This proves the absolute convergence of Equation (A-1), since $D_\phi^2 N_o$ must always be finite in any real problem.

In this analysis:

$$\left(D_\phi^2 N_o\right)_{max} = \left[(2)^2 (0.5)\right] = 2 \qquad \text{(A-21)}$$

and after 20 terms in "n", the maximum error in disregarding the 21st term is only 10% of the value of the 20th term.